UNIVERSITY OF VENDA

SCHOOL OF ENVIRONMENTAL SCIENCES

# Determination of recharge and groundwater potential zones in Mhinga area, South Africa

**By**

**Student: K.K SHAMUYARIRA (11595704)**

A Master's dissertation submitted to the Department of Hydrology and Water Resources in the School of Environmental Sciences, University of Venda, in fulfilment of the requirements for the degree of Master of Earth Sciences in Hydrology and Water Resources.

**May, 2017**

## Declaration

I, Shamuyarira K.K. declare that this dissertation for Earth Sciences in Hydrology and Water Resources at the University of Venda is my work in design and execution. The dissertation has not been submitted previously by anyone, for a degree at this university or any other university. All effort has been taken to acknowledge the material which was referenced.

……………………..                                        ……………………..

Signature                                        Date

## Abstract

This study was focused on determining groundwater recharge and groundwater potential for Mhinga area in South Africa, which is a rural area that depends mainly on groundwater for domestic water supply. Numerical modelling was used to simulate the groundwater behaviour in the aquifer and estimate groundwater recharge. MIKE SHE and MIKE 11 models were coupled and used to estimate groundwater recharge within calibration and validation periods of 2007/07/01 to 2009/12/31 and 2010/01/01 to 2013/05/21, respectively. Due to limited data availability for Mhinga, modelling was carried out at quaternary scale and then localised to Mhinga area. Remotely sensed data (satellite images, shapefiles and maps) was used to produce the groundwater potential map for Mhinga. The data were assigned with weights using Saaty's Analytical Hierarchy Process and overlain on ArcGIS platform. Borehole drilling statistics of the boreholes in A91H quaternary catchment were used to validate the groundwater potential map. In streamflow modelling using MIKE 11, values of Nash-Sutcliffe efficiency (NSE), correlation coefficient (R), root mean square error (RMSE) and mean absolute error (MAE) were 0.51-0.89, 0.73-0.97, 3.61-7.96 and 1.13-2.75, respectively. In integrated groundwater modelling using MIKE SHE, values of NSE, R, RMSE and MAE were 0.72-0.84, 0.87-0.93, 0.18-0.32 and 0.13-0.26, respectively. These values showed that MIKE SHE and MIKE 11 models had satisfactory performances. Groundwater recharge estimates were generally very low ranging from 0 to 2.75 mm/year, which constituted 0 – 0.42 % of Mean Annual Precipitation (MAP) for the A91H quaternary catchment. This was associated with high evapotranspiration (mean of approximately 4 mm/day) compared to the low precipitation levels (MAP of 656 mm/year). Moreover, in the low lying areas, with gentle slopes, low recharge between 0.2 – 0.4 mm was observed. The groundwater potential (GWP) map produced revealed that Mhinga is predominantly covered by regions of very low and low groundwater potential, which was associated with the type of geology. Area coverages of 34.47 % had very low, 51.39 % had low, 7.66 % had moderate and 6.48 % had high groundwater potential. Moderate to high groundwater potential zones were located along the geologic fault zones. In A91H, 112 unsuccessful boreholes were drilled, 69 (61.6 %) fell in the very low GWP zones, 16 (14.3 %) fell in the low GWP zones, 17 (15.2 %) fell in moderate GWP zones and 10 (8.9 %) fell in the high GWP zones. In the Mhinga, 19 unsuccessful boreholes were drilled of which, 11 (57.9%) fell in the very low GWP zones, while 6 (31.6%) fell in the low GWP zones and 2 (10.5%) fell in the moderate GWP zone. Hence 89.5% of all the unsuccessful boreholes drilled occurred in the very low to low GWP zones. It is concluded that the study area is mainly dominated by of areas with low recharge and very low to low groundwater potential. It is recommended that the MIKE SHE – MIKE 11 model and the GIS models should be developed further and improved as more data is collected to refine the conceptualisation of the aquifer.

## Dedication

The work is dedicated to The Lord Jesus Christ, for whom I live.

**Acknowledgement**

My appreciation goes to the Lord Jesus Christ. He has always held my hand throughout the research dissertation. He is the greatest supervisor and when an individual is placed under Him all will be well.

My sincere gratitude to Ms Makungo who has supervised and provided support in serious problem solving and logistics. Thanks also to Professor Odiyo for overseeing the progress of the work and his patience. Thanks to Mr Nkuna for the fieldwork supervision which he dedicated himself to.

I thank Danish Hydrology Institute of South Africa (DHI SA) for their time and tremendous assistance in guiding the MIKE 11 and MIKE SHE modelling part of this work, in particular, Mr Jason Hallowes, Bruce Eady and Andrew Pott. I also acknowledge the DHI SA for providing MIKE 11 and MIKE SHE modelling packages for free.

I thank the National Research Foundation (NRF) and the University of Venda Research and Publication Committee for funding the research dissertation. The United States Geological Survey (USGS) and South African National Space Agency (SANSA) are acknowledged for providing quality satellite images.

Special gratitude goes to my father, mother, three little sisters and the extended family. I also acknowledge my beloved Pastor Mutasa and wife, Mr Murehwa, and all the redeemable attributes of God and may others who offered prayers for the completion of this research dissertation.

Table of Contents

CHAPTER 4: GROUNDWATER RECHARGE MODELLING ........ 44

## List of Figures

## List of Tables

## Abbreviations

CMB: Chlorine Mass Balance

CRD: Cumulative Rainfall Departure

CVFE: Control Volume Finite Element

DEWA: Division of Early Warning and Assessment

DHI: Danish Hydrologic Institution

DWAF: Department of Water Affairs and Forestry

DWS: Department of Water and Sanitation

ETo: Reference Evapotranspiration

FC: Flow Characteristics

GRIP: Groundwater Resource Information Project

GUI: Graphic User Interface

GWP: Groundwater Potential

ICRC: International Committee of the Red Cross

MAE: Mean Absolute Error

MAP: Mean Annual Precipitation

NSE: Nash-Sutcliffe coefficient of Efficiency

R: correlation coefficient

RMSE: Root Mean Square Error

RS: Remote Sensing

SACS: South African Committee for Stratigraphy

SHE: System Hydrologique European

TDR: Time Domain Reflectometry

TMG: Table Mountain Group

UNEP: United Nations Environment Programme

WWO: World Weather Online

# CHAPTER 1: INTRODUCTION

## 1.1 Background

In many arid, semi-arid and rural regions, groundwater is a major contributor to total water supply (Van Camp *et al.*, 2013). Mhinga village, which is the site for this study is located in Limpopo Province of South Africa, where 70% of the total domestic water supply comes from groundwater (Du Toit *et al.*, 2012). The growing population and urbanisation, coupled with economic development is resulting in higher water uses. The rising uses and the need for water due to urbanisation and economic development, result in the doubling of water demand in every two decades (Foster and Ait-Kadi, 2012). Water is an essential need for life, which cannot be done away with, yet in reality, water is finite and vulnerable (Foster and Ait-Kadi, 2012). South Africa is semi-arid and the importance of water resources in the country is clear. This is why many towns' names have something to do with water (for example Watervaal). It has been predicted that a great scramble for water resources will occur in a few years (le Roux *et al.*, 2011).

Although South Africa has coastline areas where some saline water treatment plants have been developed, the desalination process has been found to be highly expensive. This leaves mostly freshwater, that is, groundwater and surface water as the only resources to be considered in planning and development. Of all freshwater available, groundwater constitutes 97% (Department of Water Affairs and Forestry (DWAF), 2004). Unlike surface water reservoirs, groundwater reservoirs are not usually directly recharged and can be considered finite and exhaustible. Thus, groundwater is the major contributor of freshwater yet the most vulnerable. In many cities, hydrogeological studies have been carried out for various reasons. These include minimization of saline water intrusion, determination of flow of groundwater scheme, recharge quantity and quality and declination of the water table. This has brought much knowledge and understanding of the aquifer systems, which has led to optimised abstractions, abatement, informed groundwater planning, development and allocation (Jasmin and Mallikarjuna, 2011). For this reason, many cities have adequate water supply and if the same approach could be used for rural areas, water shortages would be reduced significantly. Failure of boreholes will also be minimised as groundwater potential zones will be highlighted. Informed decisions have always proved to minimise loss of time, money and effort.

## 1.2 Statement of problem

Nkondo *et al*. (2012) pointed out that there is a lack of information regarding groundwater resources in South Africa. The quantity and quality of groundwater in most areas in South Africa is unknown. The aquifer types are only known at national level to be dominantly low yielding fractured aquifers, except in a few areas where there are dolomite and coastal sand aquifers (Nkondo *et al*., 2012). Aquifer characteristics such as recharge schemes and rates and also whether underdevelopment or overexploitation is occurring are unknown. In the management of groundwater in arid and semi-arid areas, recharge is one of the most important factors (United Nations Environment Programme Division of Early Warning and Assessment (UNEP DEWA, 2002). Shifting from the general notion that water is inexhaustible, which is untrue, the capacity of the aquifer needs to be estimated.

In many developed countries, a network of observation boreholes exists, which allows for the monitoring of groundwater levels and recharge (Van Camp *et al*., 2013). Such infrastructure is expensive, hence in contrast, rural areas in developing countries have no such networks. In most of South Africa's rural areas, including Mhinga, such infrastructure mostly does not exist. The conceptual model of the area has not been developed and there is no understanding of the aquifer system. When contamination problems in water resources arise, it is often difficult to determine contaminant source areas because of the limited understanding of recharge and subsurface flow systems in this area. The nature of aquifer systems is highly variable, hence each aquifer needs to be understood individually since knowledge of similar aquifer types cannot be used for another. There are a large number of variables affecting the aquifer systems. Individually, these are spatially variable (Jasmin and Mallikarjuna, 2011). Some of the variables are geology, precipitation, presence and depth of impermeable layers, evapotranspiration, abstractions, connectivity of aquifers, recharge source (Pradeep, 1998; Sreedhar *et al*., 2009). Short pumping tests that were done soon after borehole drilling form the little data available for the Mhinga aquifer. Where observation is not continuous a model becomes a useful tool for estimation of parameters.

## 1.3 Significance of the study

In order to make informed strategic future planning of groundwater allocation for domestic use and/or economic development, there is a need to understand its recharge and storage. A better understanding of the way an aquifer functions and the ability to assess its capacity and recharge patterns is essential because it results in the optimum and sustainable use of groundwater (Morris *et al.*, 2003). Sustainable use of groundwater is when the present day use of groundwater does not deprive future generations from enjoying the same benefits of the resource (Jha and Chowdary, 2007).

Groundwater storage in aquifers is replenished from recharge. This makes aquifer recharge one of the most important aspects of aquifer studies. A model that can forecast recharge using past trends would provide valuable information to water managers. Such information is important for regulation of abstractions, safe yield and recharge rates. Real-time monitoring is expensive and unavailable, hence a model provides approximations of hydrological variables at any given time. Mhinga is an area where very little work on groundwater assessment has been done, hence, this study will form part of the foundation on which further studies around the area can be developed.

## 1.4 Objectives of the study

### 1.4.1 Main objective

- To determine the recharge and groundwater potential zones of the aquifer in Mhinga area.

### 1.4.2 Specific objectives

- To estimate aquifer parameters of the Mhinga aquifer
- To estimate and numerically model groundwater recharge
- To delineate groundwater potential zones in Mhinga

## 1.5 Research questions

- What is the rate of groundwater recharge of the Mhinga aquifer?
- Where is groundwater found in Mhinga?

## 1.6 Characteristics of the study area

### 1.6.1 Location

Mhinga is located on the Eastern side of the quaternary catchment A91H of the Luvuvhu River Catchment in South Africa. The Mhinga area covers an area of approximately 78.1 km$^2$, lying between the longitudes 30.84$^0$ and 30.99$^0$ and latitudes 22.71$^0$ and 22.81$^0$ (Figure. 1.1).

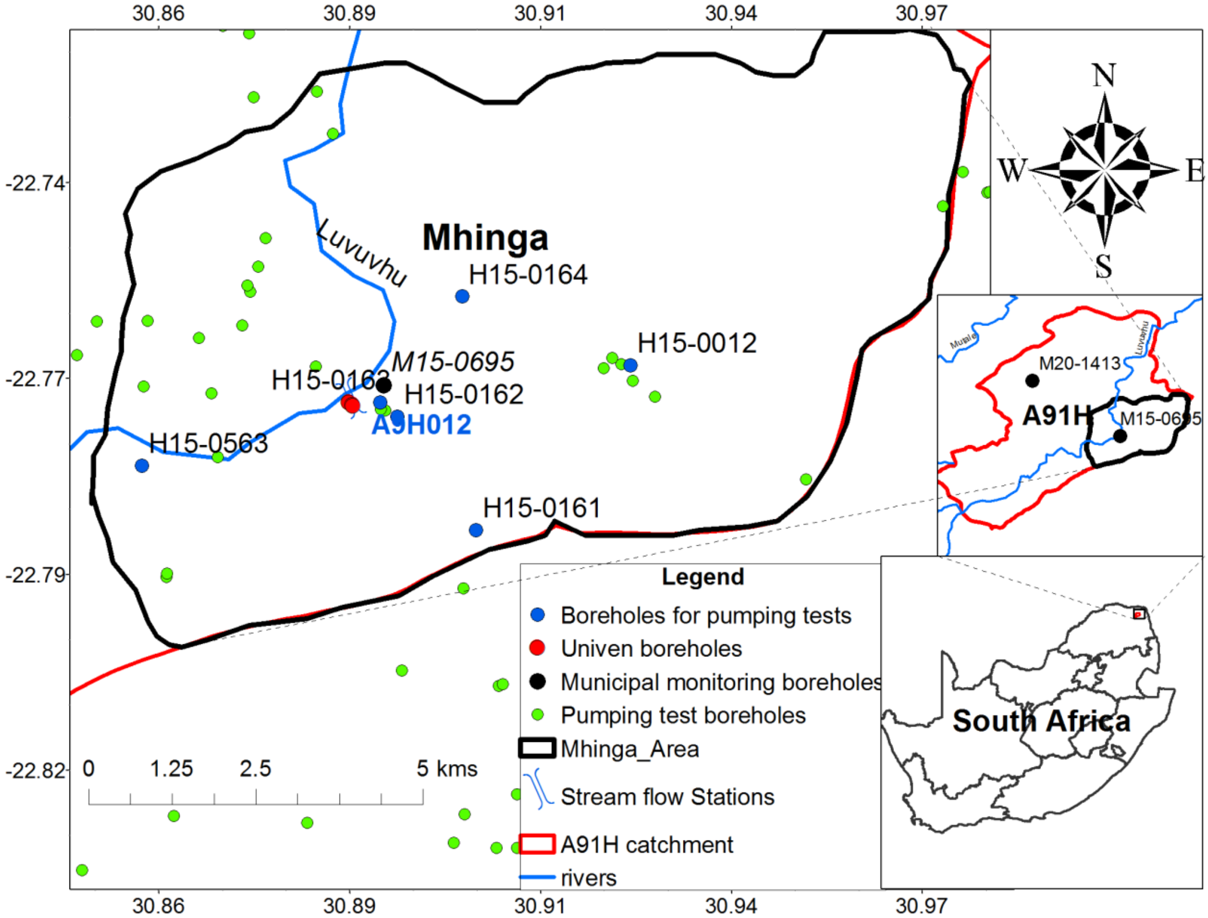


**Figure 1.1: Map of the study area**

### 1.6.2 Geology

The study area falls within the severely faulted Soutpansberg Group of the northern part of the Limpopo Province (Figure 1.2). This group comprises of a volcanic and sedimentary rock succession that is presently divided into six formations (SACS, 1980; Brandl, 1999). The Fundudzi Formation is only developed in the eastern half of the Soutpansberg Basin. The formation consists generally of sandstone with a few thin pyroclastic beds with intercalated basaltic lava at the top of the succession (Barker, 1979). The Wyllie's Poort Formation is dominated by red-pink quartzite with minor pebble washes and the base of the Formation is marked by a prominent agate pebble conglomerate (Bumby *et al*., 2002). The Formation reaches a maximum thickness of approximately 1 500 m (Barker, 1979. Basic intrusive rocks are mainly composed of dykes and sills of diabase. The dykes intruded often along fault planes and the sills were mainly emplaced along the interface of shale and competent quartzite (Bumby *et al*., 2002).

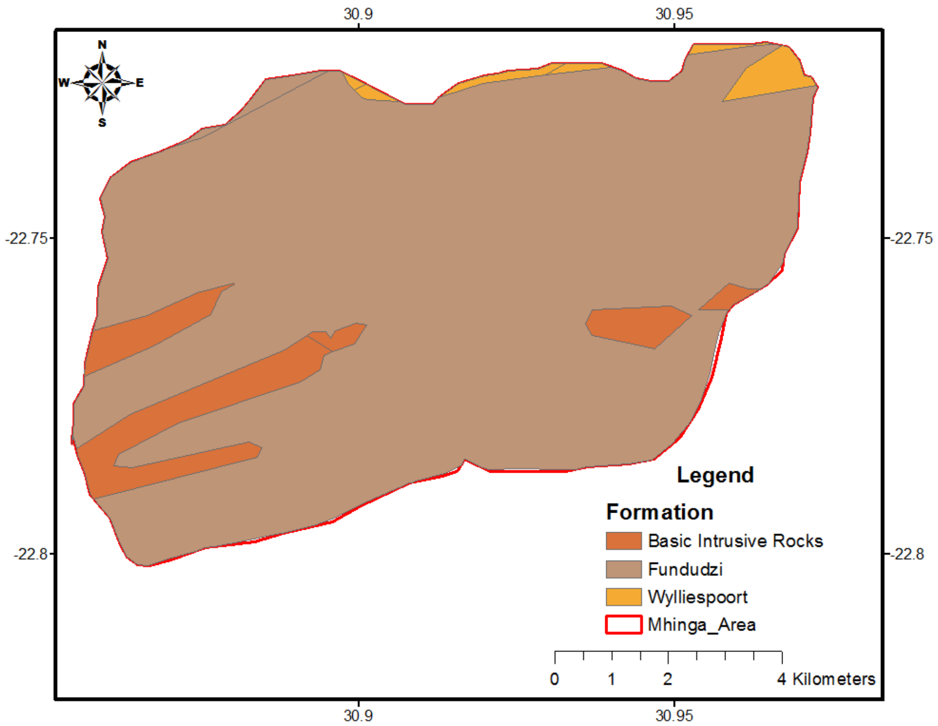


**Figure 1.2: Geological map of the study area**

### 1.6.3 Climate

The area is semi-arid, characterised by an average annual rainfall of 450 mm. Precipitation occurs during the summer season from October to March. The average daily maximum temperature is 28$^{o}$C. With such a scenario, evaporation is high when compared to precipitation (World Weather Online (WWO), 2014).

### 1.6.4 Hydrology

The Luvuvhu River, which passes through the area, drains the area (Figure 1.1). The river passes on the North western side of the area as it goes to the Kruger National Park, where it discharges into the Limpopo River.

# CHAPTER 2: LITERATURE REVIEW

This chapter provides a review of groundwater numerical modelling trends and methods. The chapter also presents methods used to analyse pumping test data. The chapter further presents literature on ways of determining groundwater potential. Since the catchment under study is in a data scarce catchment, the chapter is more biased to the indirect methods and aspects of determination of variables, which apply in such instances.

## 2.1 Hydrogeological studies

Hydrogeological studies involve studying of the characteristics of aquifers and how they influence occurrence, quality, storage and many other variables of groundwater. It has always been the desire of scientists from the beginning of mankind to look into and describe the unseen. The discovery of many underground materials, which are useful to humans has come as a by-product of hydrogeological understanding. With the growing understanding that groundwater can supplement surface water supplies, hydrogeological studies for groundwater recharge and potential have become prominent for exploration purposes.

Taylor and Greene (2006) noted that numerous geological and hydrological aspects influence the hydrogeology of an area. Some geological aspects are topography, structure and stratigraphy. The hydrological aspects identified by White (1999) necessary for the evaluation of crystalline basement aquifer systems were, area of the basin, recharge, conduit carrying capacity, hydraulic conductivity and response of the interconnected conduits. An additional aspect given is the water budget (Taylor and Greene, 2006).

Owing to the inaccessibility of underground morphology, indirect methods have been used to roughly visualise the underground morphology and processes affecting water transport and storage (Javed and Wani, 2009). Such methods are estimation, modelling and remote sensing. The use of remote sensing to obtain data for inaccessible areas and GIS for quicker and cheaper processing are becoming more useful and mandatory (National Remote Sensing Agency, 2008; Nagarajan and Singh, 2009; Thakur and Sharma, 2009; Jasmin and Mallikarjuna, 2011).

Hydrogeological studies have been done on different scales using different methods. Nguyet (2006) focused on groundwater quality. Tracer and isotope techniques were used to assess the vulnerability of Karst aquifers in a mountain area. Taylor and Greene (2006) investigated the interaction between groundwater and surface water in American aquifers by integrating existing data using GIS. Leek (2006) found that the groundwater level declines in the Palouse basin due to complex processes could not be individually pin-pointed. McLin (2007) used aquifer pump tests and borehole logs to conceptualise the hydrogeology of Guaje Canyon in Mexico. Groundwater flow characteristics of an altered aquifer were investigated by Litaor *et al*. (2008). Numerical modelling methods were used by Mondal *et al*. (2008) to evaluate pollution migration from an industrial complex in India. Groundwater quality assessment was done in a coastal area to investigate the major cause of seawater intrusion (Park *et al*., 2012).

In South Africa, a general coarse national aquifer understanding is available together with a few specific studies that have been done. Xu *et al*. (2009) conducted work on the Table Mountain Group (TMG). The study focused on using porosity, permeability and storativity properties of the aquifer to guide sustainable use of groundwater from the TMG. Van Wyk *et al*. (2012) investigated how the aquifer characteristics affected the aquifer response to rainfall events in the semi-arid regions of the Northern Cape Province. Nealer *et al*. (2009) and Pietersen *et al*. (2011) observed significant nutrient and microbial pollution in their groundwater quality studies of the Botleng and Gauteng Dolomite aquifers, respectively. The source was suspected to be sewage effluent.

## 2.2 Aquifer parameters

Aquifer parameters such as transmissivity (T), storativity (S) and hydraulic conductivity (K) are the basic information required for aquifer analysis and modelling of groundwater (Mondal *et al*., 2008). Transmissivity is the rate at which groundwater flows horizontally through an aquifer. Storativity is the volume of water released from storage per unit decline in hydraulic head in the aquifer, per unit area of the aquifer. Hydraulic conductivity is the constant of proportionality that defines fluid flows through a porous media, which is dependent on permeability and the physical properties of the media.

To estimate hydraulic conductivity, an empirical or experimental approach can be taken. Empirically, the study area’s soil texture, grain size and pore size distribution and soil mapping units are correlated with areas with known values of hydraulic conductivity. Ranges of hydraulic conductivity values for different geological formations are provided in Table 2.1.

**Table 2.1: Estimates of hydraulic conductivity (Bear, 1972)**

| *K* (cm/s) | $10^2$ | 10 | 1 | 0.1 | 0.01 | $10^{-3}$ | $10^{-4}$ | $10^{-5}$ | $10^{-6}$ | $10^{-7}$ | $10^{-8}$ | $10^{-9}$ | $10^{-10}$ |
|---|---|---|---|---|---|---|---|---|---|---|---|---|---|
| Relative permeability | Pervious | | | | Semi-pervious | | | | Impervious | | | | |
| Unconsolidated (sand & gravel) | Well sorted gravel | | Well sorted sand or sand & gravel | | | Very fine sand, silt loess, loam | | | | | | | |
| Unconsolidated (clay & organic) | | | | | peat | | Layered clay | | | Unweathered clay | | | |
| Consolidated rocks | Highly fractured rocks | | | | oil reservoir rocks | | | sandstone | | limestone, dolomite | | Fresh granite | |

Experimentally, on-site measurements such as pumping tests or laboratory measurements such as constant head and falling head can be done to determine hydraulic conductivity.

## 2.3 Pumping tests

Borehole pumping tests are usually used to determine aquifer parameters. By pumping out water at specified rates, stress is applied to the borehole and the response from the aquifer is used to estimate aquifer parameters (van Tonder *et al*., 2002). The estimated parameters are then taken as representative values for the aquifer system (Freeze and Cherry, 1979). Typically three types of such tests exist; namely, constant discharge test, stepped discharge test and recovery test. From these tests, Theis and Cooper-Jacob formulas can be applied to estimate aquifer parameters. Factors affecting the choice of pumping test are provided in Table 2.2. The choice of formula to be used depends on the type of aquifer, whether confined or unconfined (Freeze and Cherry, 1979).

**Table 2.2: Factors affecting choice of pumping test (adapted from International Committee of the Red Cross (ICRC), 2011)**

| Type of test | Parameters derived from the test (using simple methods of analysis) | Typical length of the whole test | Limitations of the test |
|---|---|---|---|
| Step test | Specific drawdown<br>Specific capacity<br>Qualitative assessment of borehole performance<br>Pumping rate for constant-rate test | 1 day | Must be able to vary the pumping rate.<br>Not reliable when predicting long-term aquifer behaviour |
| Constant-rate test | Aquifer transmissivity<br>Storage coefficient, if observation borehole is there<br>Qualitative assessment of ability to maintain the planned yield | From 1 day up to 2 weeks | Difficult to keep the pumping rate constant<br>Aquifer parameters may be different in wet season compared to dry season<br>Must have good discharge system |
| Recovery test | Aquifer transmissivity<br>Qualitative assessment of well losses (related to borehole efficiency) | Several hours to days | A foot-valve must be fitted to the rising main<br>Pump cannot be removed during test |

### 2.3.1 Stepped discharge test

Stepped discharge tests are used to estimate borehole efficiency and optimum yield. The borehole is subjected to pumping in equal time steps. After every time step, which is usually 1 or 2 hours, the pumping rate is increased by a fixed increment. An example of the stepped discharge test is provided in Figure 2.1. The stepped test is good for determining the short-term relationship between yield and drawdown of a borehole. The test is limited to determine borehole and not aquifer characteristics. Hence the stepped test usually foreruns and provides estimation data for the constant discharge test (ICRC, 2011).

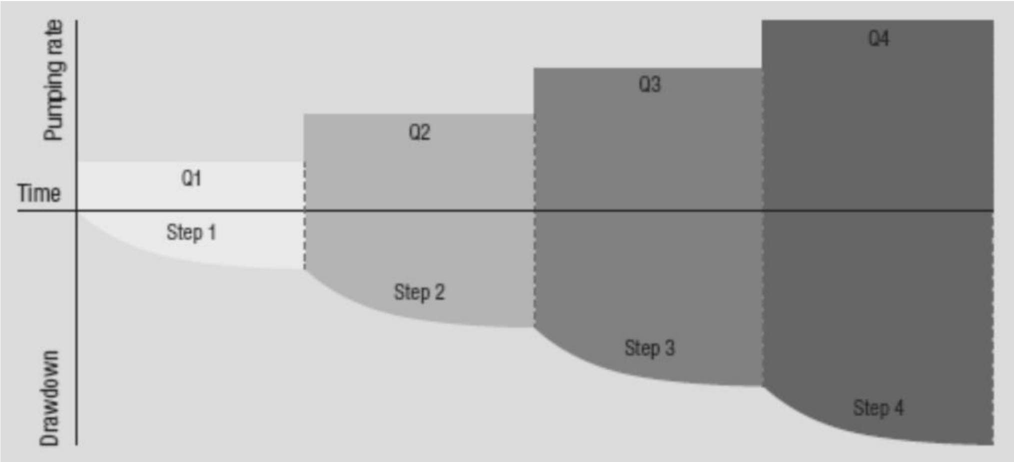


**Figure 2.1: Graphical representation of a step discharge test adopted from ICRC (2011)**

### 2.3.2 Constant discharge test

Constant discharge tests are carried out in order to estimate aquifer parameters, nature and boundaries (Hiscock, 2005). These are the pumping tests used in aquifer analysis. The borehole is subjected to prolonged pumping, for 12 to even 72 hours, at a constant sustainable rate.

For both tests, a plot of time vs. drawdown is made, which is then matched with the Theis (1935) type curve or the Cooper-Jacob (1946) straight line solution. From the curve matching, T and S can be determined.

$$s = \frac{2.3Q}{4\pi T} log \frac{t_2}{t_1} \qquad (2.1)$$

Where $s$ is the drawdown, $T$ is transmissivity, t is time and $Q$ is discharge of the well.

But when $log\,\frac{t_2}{t_1} = 1$, $\Delta s$ is drawdown difference per log cycle, then the equation rearranges to

$$T = \frac{2.3Q}{4\pi\Delta s} \qquad (2.2)$$

Storativity ($S$) is given by

$$S = \frac{2.25Tt_0}{r^2} \qquad (2.3)$$

Where $t_0$ is the value of t at the intercept and $r$ is the distance from the discharging well

### 2.3.3 Recovery test

After pumping is stopped, the water levels in the borehole and aquifer start to rise again which is called recovery or residual drawdown (Freeze and Cherry, 1979). Aquifer parameters can be estimated from the rate and pattern of recovery (Hiscock, 2005). The recovery test is more reliable than the other two because recovery takes place at a constant rate while on the other hand, it is very difficult to maintain a constant pumping rate in the real field. The recovery test is also usually used to verify the aquifer parameters estimated in the constant rate test (ICRC), 2011). The Theis (1935) equation used to estimate transmissivity (T) is as follows

$$T = \frac{2.3Q}{4\pi\Delta s\prime} \qquad (2.4)$$

Where, Q is the rate of discharge in $m^3$/day and $\Delta s'$ is the residual drawdown difference per log cycle of t/t' (t is time from beginning of pumping and t' is time from the end of pumping in m).

## 2.4 Estimation of groundwater recharge

In the management of groundwater resources, one of the most important parameters is recharge; though it is one of the most difficult parameters to estimate. This difficulty arises from the fact that recharge is influenced by many factors, which are extremely spatially variable. Some of the factors are geology, topography, abstractions, precipitation, evapotranspiration, land use and infiltration rates (UNEP DEWA, 2002). To make it worse, in crystalline/consolidated aquifer conditions, there is more heterogeneity because the storage and transmission of water depend on secondary porosity only, due to fissures, cracks and openings in the crystalline rocks, which are usually randomly distributed. In unconsolidated aquifer material, in contrast, there is primary porosity due to the geological material composition and secondary porosity due to fissures, cracks and openings caused by physical and chemical weathering of geologic material (Meyer, 2002). Hence aquifer recharge in unconsolidated aquifers is less complicated compared to consolidated/crystalline aquifers. There are several methods for estimating groundwater recharge. These can be classified into two classes.

- Physical methods

Direct measurements - These include the measurement of soil moisture content using instruments such as Lysimeters, Neutron and Time domain reflectometry (TDR) probes. The estimates obtained can be used to calibrate models in the other recharge estimation techniques. The limitation is that the results produced are locally based for a specific soil type or structure and vegetation. In arid areas, recharge depends on individual recharge features and is not areal or uniform, which might render this method inapplicable (UNEP DEWA, 2002).

Water balance techniques - The technique is similar to book-keeping in accounting terms. Water input and water output/discharge are compared and the difference in the two is the estimated recharge (UNEP DEWA, 2002). Water input can be precipitation and water discharge can be actual evapotranspiration, runoff and abstractions. This method was developed in 1948 by Thornthwaite and has been further developed from there. The basic equation to get recharge (R) is,

$$R = P - E_a \pm \Delta W - R_0 \quad (2.5)$$

Where P is precipitation, $E_a$ is actual evapotranspiration, ΔW is change in soil water storage and $R_0$ is runoff. Some of the methods included in this class are soil moisture budgets, cumulative rainfall departure (CRD), river Channel Water Budget (CWB), water table Fluctuation (WTF), Hydrograph Separation (HS) and Saturated Volume Fluctuation Departure (SVF) methods (Table 2.3). Water balance methods are inaccurate, although they are easy to calculate. Inaccuracy arises because recharge is a difference of precipitation and evaporation whose estimations are inaccurate individually. The resulting error is therefore high.

**Table 2.3: Physical methods of estimating groundwater recharge (adapted and edited from Xu and Beekman, 2003)**

| Approach | Zone | Method | Principle | References |
|---|---|---|---|---|
| Physical | Surface water | HS | Stream hydrograph separation: outflow, evapotranspiration and abstraction balances recharge | Xu *et al.*, 2002 |
| | | CWB | Recharge derived from difference in flow up-stream and downstream accounting for evapotranspiration, in and outflow and channel storage change | Lerner *et al.*, 1990 |
| | | WM | Numerical rainfall-runoff modelling; recharge estimated as a residual term | Sami and Hughes, 1996 |
| | Unsaturated | Lysimeter | Drainage proportional to recharge | Bredenkamp *et al.*, 1995 |
| | | UFM | Unsaturated flow simulation e.g. by using numerical solutions to Richards equation | Lerner et al., 1990 |
| | | ZFP | Soil moisture storage changes below ZFP (zero vertical hydraulic gradient) proportional to recharge | Gieske, 1992 |
| | Saturated | GM | Recharge inversely derived from numerical modelling of groundwater flow and calibrated on groundwater ages | Gieske, 1992 |
| | | SVF | Water balance over time-based on averaged groundwater levels from monitoring boreholes | Bredenkamp *et al.*, 1995 |
| | | EV-SF | Water balance at catchment scale | Bredenkamp *et al.*, 1995 |
| | Integrated (Unsaturated + saturated) | CRD | Water level response from recharge proportional to cumulative rainfall departure | Xu and Van Tonder, 2001 |
| | | EARTH | Lumped distributed model simulating water level fluctuations by coupling climatic, soil moisture and groundwater level data | Van der Lee and Gehrels, 1997 |
| | | WTF | Water level response proportional to recharge | Bredenkamp *et al.*, 1995 |

D'Arcyan techniques - Such techniques use the variation in head gradient and hydraulic conductivity to estimate recharge. D'Arcyan techniques can be applied in the saturated (phreatic) zone or the unsaturated (vadose) zone of the underground geology. In the unsaturated zone, recharge estimates can be obtained from measurements of matrix potential and solving Richard's equation. In the saturated zone, recharge estimates can be obtained from pumping tests and head measurements. Importantly, numerical models are usually used to estimate recharge using D'Arcyan techniques. Water models (WM) and Groundwater Models (GM) may be used in both saturated and unsaturated zones individually or coupled, depending on the input data available.

- Tracer methods

These techniques involve the introduction of dissolved substances or solutions into the water cycle and then tracing the movement of water using their concentrations. Common tracer methods are Chloride Mass Balance (CMB) and Groundwater dating (GD) (Table 2.4).

**Table 2.4: Tracer methods of estimating groundwater recharge (adapted from Xu and Beekman, 2003)**

| Approach | Zone | Method | Principle | References |
|---|---|---|---|---|
| Laser | Unsaturated | CMB | Chloride Mass Balance – Profiling: drainage inversely proportional to Chlorine in pore water | Beekman *et al.*, 1996 |
| | | Historical | Vertical distribution of tracer as a result of activities in the past ($^{3}H$) | Gieske, 1992 |
| | Saturated | GD | Age gradient derived from tracers, inversely proportional to recharge; Recharge unconfined aquifer based on vertical age gradient ($^{3}H$, CFCs, $^{3}H/^{3}He$); Recharge confined aquifer based on horizontal age gradient ($^{14}C$) | Weaver and Talma, 1999 |
| | Integrated (Unsaturated + saturated) | CMB | Amount of Cl into the system balanced by amount of Cl out of the system for negligible surface runoff | Selaolo, 1998 |

Tracing can be done either using environmental or artificial tracers. The source of environmental tracers is natural or anthropogenic and they are introduced into the water cycle over a long time. Artificial tracers are applied for tracing purposes over a relatively short time and in a small area. On the other hand, natural tracers are able to trace average water movements over a long time. Chloride, tritium, tritium-helium 3 and carbon 14 are examples of tracers.

### 2.4.1 Groundwater numerical models

In this study, an integrated numerical modelling approach has been used in a semi-arid area with limited data. The choice comes after recognition that successful estimation of groundwater recharge requires an integrated approach as explained in UNEP DEWA (2002). The underground is relatively inaccessible, hence there arises the need to model from the little available data obtained from drilled boreholes and lineaments. Because of the many variables involved, a model is helpful in that it can combine many types of data (images, maps, hydrogeological and meteorological parameters, temporal data, etc.) and come up with an estimate and a rough picture of the unseen. The more data you put in, the closer the model is to the real situation and the more accurate it is.

There is a vast array of numerical model codes, which can be used for groundwater modelling. In terms of conceptualization, a hydrological model can be lumped, distributed or semi-distributed. A lumped model is one in which the catchment is regarded as one unit and the flow characteristics are averaged to obtain single values representing the catchment (Mook, 2001). On the other hand, a distributed model takes into account all variations in space. In a semi-distributed model a few variables are kept constant or lumped and the majority are allowed to vary spatially (Garraway *et al*., 2011).

In terms of simulation results, hydrological models can be stochastic or deterministic. Generally stochastic models can be used to investigate the effects of uncertainty and reduce noise while deterministic models are used to investigate the effects of change inputs. Deterministic models can be classified into three: empirical, physical and conceptual. The empirical model is based on mathematical relationships between inputs and outputs. The model does not take account of the processes taking place in the compartments through, which the water passes. In calibrating, the model parameters are adjusted until the simulated values match acceptably with the observed ones. Hence empirical models are simple and take a short time to run, compared to other types. They find application in cases where quick, average and bulk estimates are required. The challenges associated with them are that they cannot estimate local scale features and the quality of their estimates depreciates significantly when the model is applied to a different catchment (UNEP DEWA, 2002).

Physically based types of models are majorly dependent on the physical processes that affect the catchment in question. Most of the model inputs are obtained from field measurements. Compared with empirical and conceptual models, physical models require less historical data but more current field measurements and simulation time. The physical processes are represented in terms of mass, energy and momentum. The terms are represented by partial differential equations, which are then linked and solved. Most groundwater and surface water modelling is currently physically based (Garraway *et al*., 2011).

In a conceptual model, a combination of equations, physical structures and empirical relationships are used. The input data is not entirely from field observations but most data is obtained indirectly from calibration. Like the empirical type, historical data records are useful for simulation and the simulation periods are shorter than for physically based models (Garraway *et al*., 2011).

### 2.4.2 Models Review

Examples of outstanding physically based, deterministic models are Groundwater and Surface-water flow (GSFLOW), HydroGeoSphere, Parflow, Modular hydrologic modelling system (MODHMS) and MIKE System Hydrologique European (SHE) (Garraway *et al*., 2011). They are outstanding in that they are integrated, distributed, have records of publication, have been used by non-development team members, have been tested and have detailed documentation.

**GSFLOW** is a groundwater model, which is physically-based and semi-distributed. In GSFLOW, the groundwater model, MODFLOW (Harbaugh, 2005), is coupled with the surface water model, PRMS (Precipitation-Runoff Modelling System) (Leavesley *et al*., 1983). The model code is configured in a way that it solves between three regions of the water cycle, the land region, the surface region and the groundwater region (Markstrom *et al*., 2008). The regions interact by exchanging solved components like inflow and discharge amongst each other. The land and surface regions are solved by the PRMS code and this is done by dividing precipitation into overland runoff, evapotranspiration, interflow and groundwater recharge. Immediately, the water infiltrates PRMS links to MODFLOW and the latter code takes over. MODFLOW solves unsaturated groundwater flow using the kinematic wave approximation of Richard's Equation and the saturated groundwater flow using the 3D flow partial differential equation with constant density (Markstrom *et al*., 2008; Garraway *et al*., 2011).

**HydroGeoSphere** (HGS), like GSFLOW, is a physically-based and distributed model. It is formed as a full integration of the surface water model MODHMS into the model FRAC3DVS, which is for saturated zone flow of groundwater (Therrien *et al*., 2004). The surface flow is represented using St. Venant equations under two-dimensional diffusive wave approximation. D'arcyian and Richard's equations are applied to the sub-surface conditions. The same approach is employed by MODHMS and Parflow models in dealing with surface and subsurface conditions. HGS has the advantage of simulating effects of structures and micropores, which are the major sources of groundwater in basement aquifers. The computation in HGS is done using the Control Volume Finite Element (CVFE). This solver hybridises the advantages of both the finite difference and finite element methods. It deals with irregular boundaries using the finite element method and uses superior local mass capacity of the finite difference method. HGS uses adaptive time steps. This also reduces simulation effort and time required (Garraway *et al*., 2011).

**MODHMS** is a model which was developed from the USGS unsaturated groundwater model, MODFLOW-SURFACT. The model shares similarities with HGS and Parflow in the treatment of surface and subsurface conditions. Added to the advantage of adaptive time stepping regime, MODHMS can simulate hydraulic structures like weirs and dams, which is not possible in HGS and Parflow. Another advantage is that MODHMS has an interface with ArcView GIS and a well-designed Graphic User Interface (GUI) for the subsurface, these tools are very useful in model parameterization (Weber *et al*., 2004). The model is well documented and also continually updated (Jones *et al*., 2003; Panday and Huyakorn, 2004). Disadvantages include inflexibility in terms of representing hydrological processes occurring at different complexity levels, longer simulation periods due to the single processor design (Garraway *et al*., 2011).

**Parflow** is a model which was originally developed for groundwater research. In recent years, processes in surface flow have been incorporated making the model to be integrated. Parflow is solved using the finite difference method and the same equations for the surface and subsurface conditions as HGS and MODHMS. The model can be linked to many other models because it is very modularized or made into many separate parts, which can be simulated together. Having been originally developed for research purposes in water transport, Parflow lacks important tools for water resource management such as GIS integration, GUI and hydraulic structure simulation. Additional software is required to visualise the output (Kollet and Maxwell, 2006).

**MIKE SHE** is a very flexible model code in terms of the amount of data, type of data and simulation methodologies. All processes are calculated on a uniform grid basis except for channel routing. Surface water is portioned into two, overland flow and streamflow. The overland portion can be simulated using either lumped or distributed methodology. Streamflow generated is dealt with by linking MIKE SHE to MIKE-11 model in a bi-way. Subsurface flow is also partitioned into saturated zone flow and unsaturated zone flow and these are simulated separately (Camp Dresser and McKee Incorporated, 2001; Gordon *et al*., 2005). For saturated flow either a lumped linear reservoir approximation method or Darcy equation can be used. The linear reservoir method is an over simplified type of the system, neither simulates flow nor interaction between groundwater with surface water. Using the implicit finite difference method to get the solution of the saturated zone 3D Darcy equation offsets these limitations (Weber *et al*., 2004).

MIKE SHE is equipped with a well-designed GUI and allows importation and integration of various types of data, and results-viewing, unlike the other models which have a few sets of data types, which they are compatible with. MIKE SHE is also equipped with a toolkit for ArcView GIS which can be used alternatively for parameterisation (Garraway *et al*., 2011).

### 2.4.3 Choice of a model code

GSFLOW, HydroGeoSphere, Parflow, MODHMS and MIKE SHE models codes are appropriate to model groundwater recharge according to Garraway *et al*. (2011). In the choice of a model code, factors that were considered are credibility, flexibility and cost. MIKE SHE has the best interface of the five model codes. Although HydroGeoSphere is the least costly, followed by MODHMS, and MIKE SHE is the most expensive. GSFLOW and Parflow can be downloaded for free. The advantage of the commercial codes is that they are constantly improved, and training and assistance are readily available. Apart from MIKE SHE, the reviewed model codes have been designed to be used on single processor computers. This design limits them from using the modern multi-core processor computers to reduce run times. The other advantage of MIKE SHE over the other models in this review is its flexibility in terms of representing hydrological processes occurring at different complexity levels. MIKE SHE has the longest record of use when compared to other integrated water flow models in this review (Thompson *et al*., 2004; Hansen *et al*., 2007; Vazquez *et al*., 2008). MIKE SHE code was selected for use in this study based on the above mentioned advantages. The licence was made free available for this study by DHI South Africa because of a memorandum of understanding signed with University of Venda.

MIKE SHE is a distributed physical model which takes into account all processes which take place in the hydrological cycle. The major processes include precipitation, evapotranspiration, infiltration, groundwater recharge, aquifer interflow, groundwater discharge and surface runoff. In the MIKE SHE model, there are different options of algorithms available to approximate these processes. Detailed model description can be found in Refsgaard and Storm (1995) and DHI (2012).

## 2.5 Groundwater potential zonation

Before the incorporation of remote sensing (RS) techniques, groundwater potential studies were only done using data from field observations (Marghany *et al*., 2009). Such data included pumping test data, cross-sections' data, and eye observations. The processes of collecting such data were time-consuming and expensive. Another setback was that these techniques were only able to cover small areas of land, whereas processes affecting aquifers occur over large areas of land. RS in the form of aerial photography, satellite imagery and geophysics evolved as solutions with larger coverage, lesser collection period and access to physically inaccessible areas (Lyle and Stutz, 1983). The World Wars and the lunar activities amplified the advance in remote sensing techniques (Lillesand, 1990). In characterising the moon's surface, James and Hedenquist (1978) used RS. RS became useful in environmental exploration studies from the late 1970s to date. Remote sensing is, without doubt, the backbone of hydrogeological reconnaissance in areas of the world where the coverage of detailed geological maps and field data is insufficient (Hoffmann and Sander, 2007).

Having obtained field observation data sets, traditional interpretation and mapping were also highly demanding on time and money (Aboyeji *et al*., 2012). There arose a need for a platform on which the various sets of data could be integrated and analysed. Geographical Information Systems (GIS) was used by Hill *et al*. (1983) to manipulate environmental data. Gimblett (1989) reviewed the benefits of using GIS in simulation and modelling of the earth's surface. Robinson *et al*. (1989) used and discussed the evolution of GIS and RS integration. This was of major importance and expanded the scope of groundwater potential mapping (Mogaji *et al*., 2012). Sander (2007) further illustrates such importance when hard rock terrains are involved. GIS has progressed concurrently with computer technologies. As faster computer processors were developed, GIS increased in its capability to analyse various complex and varying data. In hard rock aquifer studies by Machiwal *et al*. (2011) and Vasanthavigar *et al*. (2011), eight and four different data sets, respectively, were assessed on a GIS platform. Geology, geomorphology, soil, lineament, land-use drainage, slope and rainfall data were mainly used to make thematic maps. In both of these, overlaying of the available thematic maps produced the groundwater potential maps. The groundwater potential maps they generated were found to be reliable, as confirmed by the borehole yields.

## 2.6 Factors influencing groundwater potential

### 2.6.1 Land Use/ Land Cover (LU/LC)

The role of Land use/ Land cover (LU/LC) on groundwater potential is obvious and wide. Types of land cover/ land use are forest plantations, crop farms, open denuded soils surfaces, water bodies like lakes and rivers and settlements. Each LU/LC has a certain influence on groundwater potential indirectly through infiltration, runoff and evaporation (Fashae *et al*., 2013; Sreela *et al*., 2013). Vegetation cover minimises evaporation and runoff while it increases infiltration. Hence vegetation increases chances of groundwater recharge and can be an indication of high groundwater potential (Leduc *et al*., 2001). Forest plantations require large amounts of water, which they abstract from the vadose zone and in other cases from beneath the water table hence forest plantations indicate high groundwater potential. In settlements and built up areas, infiltration is low because of roads, pavements and buildings covering the soil surface and consequently, low groundwater potentials are expected (Sreela *et al*., 2013).

### 2.6.2 Geomorphology and slope

Avinash *et al*. (2011) demonstrated that geomorphology is a good proxy for groundwater potential analyses. The landform and landscape features are well-reflected by geomorphology. The slope is a type of geomorphological feature, which highly influences groundwater infiltration and recharge. Where steep slopes are present, groundwater potential is low because there is more surface runoff than infiltration (Fashae *et al*., 2013). In areas characterised by flatlands and/or valleys, groundwater potential is high because it is easier for the water to form pools and infiltrate than to runoff on the surface. In the study of Pradhan (2009), geomorphology was the theme with the highest weight of 0.485 in the GIS integration of thematic maps.

### 2.6.3 Geology

It is common knowledge in the field of hydrogeology that geology influences groundwater movement, storage and subsequently, potential. In a study on three sites by Krishnamurthy *et* *al*. (1996), it was noted that geology is also a major theme in groundwater analysis. A study by Pradhan (2009) also assigned the second highest weight to the geology of all the themes used for groundwater zonation in Bharangi River basin, India.

### 2.6.4 Lineaments

Lineaments are linear features, which occur on the earth's surface, distinct from the surrounding features, and reflect what the unseen subsurface can be (O'Leary *et al*., 1976). Examples of lineaments are joints, faults, fracture zones, dykes, lithological contacts and foliations (Holland, 2011; Mogaji *et al*., 2012). It has become prominent throughout the last few years to use lineaments studies in the assessment of potential groundwater zones. Jha *et al*. (2007) and Sander (2007) pointed out a number of studies in which exploration and assessment of groundwater resources were done using lineaments mapping as a core of the exploration. Furthermore, Morelli and Piana (2006) studied the correlation between structures mapped in the field and those mapped using the lineament technique. They found a high correlation, which therefore allows the structures of an area to be indicated by lineaments.

### 2.6.5 Soil

Infiltration and, consequently, groundwater, is highly dependent on the type of soil and soil texture. Sandy soil has large particle constituents, which makes it have high transmissivity and infiltration values. On the contrary, clay soils have small particle constituents, resulting in low transmissions. In terms of groundwater potential, sandy soils are assigned higher weights, clay soils are assigned lower weights and loamy soils are assigned intermediate weights (Jha *et al*., 2010; Magesh *et al*., 2012; Avinash *et al*., 2011; Fashae *et al*., 2013).

### 2.6.6 Rainfall

Groundwater recharge mainly comes from rainfall. Rainfall is a major hydrological parameter which influences groundwater potential and viability (Avinash *et al*., 2011). In areas where fossil groundwater is available, rainfall may not indicate groundwater potential but it will indicate sustainability of groundwater exploitation and can be used to estimate optimum water extraction levels.

### 2.6.7 Proximity to drainage

The areas surrounding water bodies such as lakes and rivers usually have high groundwater levels due to the lateral flow of water. Hard rock aquifers close to water bodies might have little groundwater difference from alluvial areas, which are more isotropic in nature. This is because, in hard rock aquifers, which are likely to be found in the study area, the flow of water is dependent on fissures and conduits. Closer proximity to the drainage network means that probability of finding groundwater is high (Fashae *et al*., 2013). Moving away from the drainage, the groundwater potential decreases. Groundwater movement is very slow, hence at an imaginary threshold proximity to drainage, the influence of the drainage becomes insignificant.

# CHAPTER 3: RESEARCH METHODOLOGY

This chapter explains how the groundwater recharge and groundwater potential studies of the Mhinga area were carried out. Since the methods of accomplishing each objective were different, each objective was approached individually in terms of data requirements, methods of analysis and materials. The main data requirements were on the subsurface; borehole logs, water levels and samples for water quality analysis, and on the surface; maps, satellite images and weather records, etc. The study was mainly based on already available data sets and a small fraction of data, which was measured and acquired.

## 3.1 Estimation of aquifer parameters

In the study, pumping test data for pumping tests which were carried out just after construction of water supply boreholes was used. These data were obtained from Department of Water and Sanitation (DWS). A simple programme called Flow Characteristics (FC) was used to calculate and graphically represent S and T.  FC uses several different formulae, including the Theis (1935) and Cooper-Jacob (1946) solutions to calculate hydraulic conductivity, transmissivity and storativity from pumping test data. The programme is in the form of a Microsoft Excel Spreadsheet, which when fed with pumping test data, it automatically/simultaneously calculates the aquifer parameters. The FC programme was used to estimate aquifer parameters in the Free State Province and the results were in agreement with a 3-D model used (Van Tonder *et al*., 2001). The advantage of the FC programme is that it is not data intensive, which makes it useful in data scarce areas. The FC programme is also beneficial because it has many methods of analysis in it for the variety of conditions which characterise an area. The Limpopo Groundwater Resource Information Project (GRIP) project used the FC programme to enhance the groundwater database by analysing pumping tests data from over 2000 boreholes (Holland, 2011). The estimated aquifer parameters were essential for and were used in groundwater recharge modelling.

## 3.2 Groundwater recharge modelling

MIKE 11 surface water model was used to simulate streamflow while MIKE SHE model was used to model groundwater recharge for the Mhinga aquifer based on the reasons specified in section 2.4.3.

### 3.2.1 MIKE 11 and MIKE SHE data requirements

Data required for MIKE 11 channel model and MIKE SHE groundwater recharge model included spatial (topography, Land use, soil types), hydrogeological (geological profiles, maps, streamflow measurements, groundwater levels) and meteorological (rainfall, wind, temperature) datasets. MIKE 11 and MIKE SHE modelling were done at quaternary catchment scale due to the limited data for the Mhinga area.

**Topography**

A Digital Elevation Model (DEM) was used to specify topographical data of the A91H quaternary catchment. The DEM was generated by Inverse Distance Weight (IDW) interpolation of a 50 m contour line shapefile using ArcGIS 10.2. The final resolution of the DEM was set to 100 m.

**Land use**

A land use classification file provided by DHI South Africa was used. In the file, the land uses were categorised into 13 main classes (Figure 3.1). The land use file included for each land use type, Leaf Area Index (LAI) values, Root Depth (RD) and evapotranspiration parameters from literature and past modelling experiences by DHI.

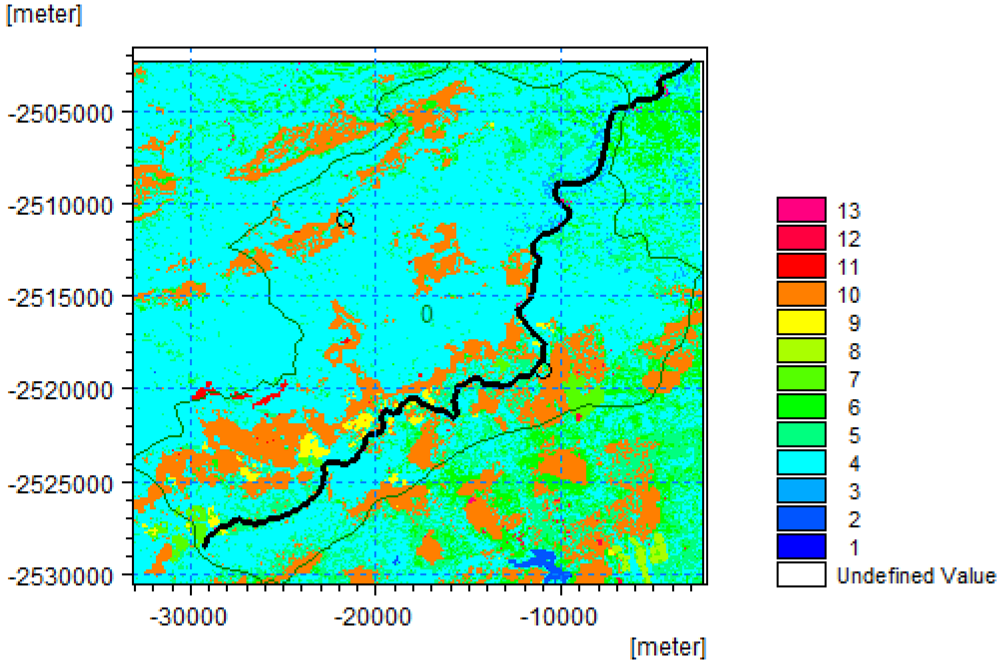


**Figure 3.1: Land uses**

**Legend**

1. Water seasonal
2. Water permanent/Wetlands
3. Indigenous Forest
4. Thicket /Dense bush
5. Woodland/Open bush
6. Grassland/Low shrubland
7. Cultivated comm fields (high)/Cultivated comm fields (med)/Cultivated comm fields (low)
8. Cultivated comm pivots (high)/Cultivated comm pivots (med)/Cultivated comm pivots (low)
9. Cultivated orchards (high)/Cultivated orchards (med)/Cultivated orchards (low)
10. Cultivated subsistence (high)/Cultivated subsistence(med)/Cultivated subsistence(low)/Urban village (dense trees / bush)/Urban
11. Plantations / Woodlots mature/Plantation / Woodlots young
12. Mines 1 bare/Mines 2 semi-bare/Erosion (donga)/Urban village (bare)/Urban built-up (low veg / grass)
13. Bare none vegetated/Urban commercial

### Soil types

The soil data was supplied by DHI South Africa. In the dataset, the unsaturated zone was characterised by parameters such as wilting point, field capacity, saturation point, saturated hydraulic conductivity and suction at wetting front (Table 3.1). The two-layer approach uses the Green and Ampt method to estimate infiltration to the unsaturated zone. Water percolates into the water table when soil moisture is more than field capacity.

**Table 3.1: Soil properties (Source: DHI South Africa)**

| Soil ID | Water content at saturation | Water content at field capacity | Water content at wilting point | Saturated hydraulic conductivity (m/s) | Soil suction at wetting front (m) |
|---:|---:|---:|---:|---:|---:|
| 40.7 | 0.43 | 0.23 | 0.15 | 1.20E-01 | -0.20 |
| 51.1 | 0.42 | 0.25 | 0.19 | 1.20E-05 | -0.20 |
| 55.8 | 0.41 | 0.30 | 0.24 | 1.20E-05 | -0.20 |
| 59.4 | 0.44 | 0.22 | 0.14 | 1.20E-01 | -0.20 |
| 60.1 | 0.44 | 0.23 | 0.15 | 1.20E-05 | -0.20 |
| 62.9 | 0.44 | 0.23 | 0.15 | 1.20E-05 | -0.20 |
| 68.8 | 0.45 | 0.21 | 0.12 | 1.20E-05 | -0.20 |
| 89.1 | 0.45 | 0.20 | 0.11 | 1.20E-05 | -0.20 |
| 94.3 | 0.45 | 0.23 | 0.15 | 1.20E-01 | -0.20 |
| 106.6 | 0.45 | 0.21 | 0.12 | 1.20E-05 | -0.20 |

### Hydrogeological data

Hydrogeological data were scarce for the A91H catchment. The data used were the daily groundwater levels, pumping tests and hydrogeological maps. Geological profiles were obtained from borehole drilling logs for the monitoring boreholes. The hydrogeological maps (DWAF, 2006) provided coarse scale data on aquifer yields and aquifer types. Hourly water levels from the groundwater monitoring points in Figure 3.2 were obtained from DWS.

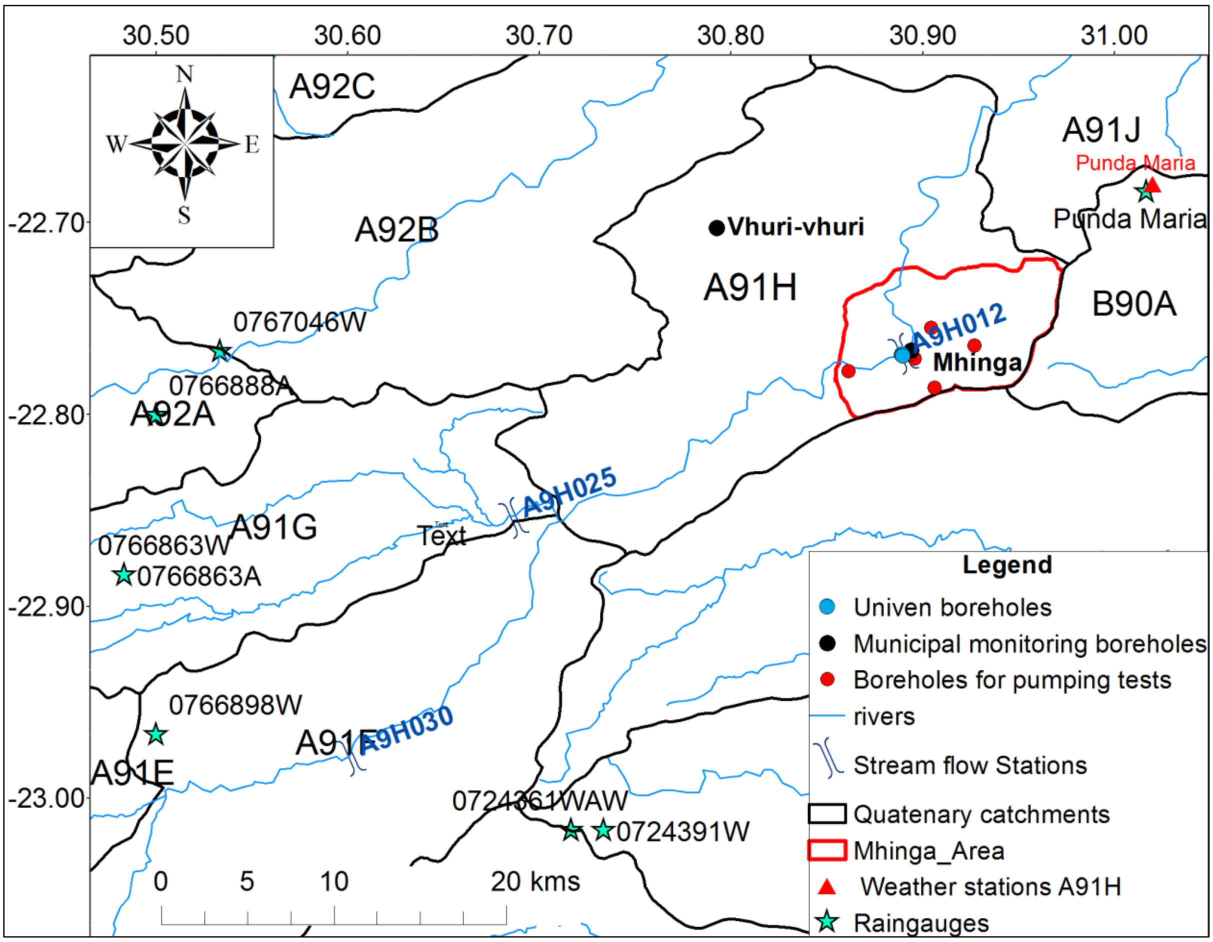


**Figure 3.2: Location of data monitoring points**

**Meteorological data**

In A91H quaternary catchment there was no weather station with rainfall, wind speed and minimum and maximum temperatures data recordings for the simulation period. Reliable daily rainfall data was only available for Punda Maria station (0768011A8) and this was used to represent the quaternary catchment. Punda Maria station is in the neighbouring quaternary catchment (B90A). Wind speed and temperatures data were also collected from Punda Maria weather station on account of the station being reasonably closer to A91H than all the other weather stations or independent raingauges located outside A91H (see Figure 3.2).

Streamflow time series

Streamflow data for A91H catchment was supplied by DWS for the three stream gauges A9H030, A9H025 and A9H012. Stream gauges A9H030 and A9H025 are located on the upstream outside of A91H while A9H012 is located in Mhinga inside A91H. A9H030 is located on the Mutshundudi River, which is the last tributary of Luvuvhu River before it enters A91H quaternary catchment while A9H025 and A9H012 are on the Luvuvhu River (Figure 3.2). The streamflow data were approximately 8 to 27 years long at a daily time step. The data for A9H025, A9H012 and A9H030 were from November 1995 to May 2015, December 1987 to December 2014 and June 2007 to May 2013, respectively.

### 3.2.2 Model domain and discretisation

Model simulations were performed at six-hour time steps using grid size or spatial resolution of 100 m. The model domain consisted of the whole A91H quaternary catchment with approximately 449.9 $km^2$ of area (Figure 3.3). The model grids were discretised to 100 m by 100 m.

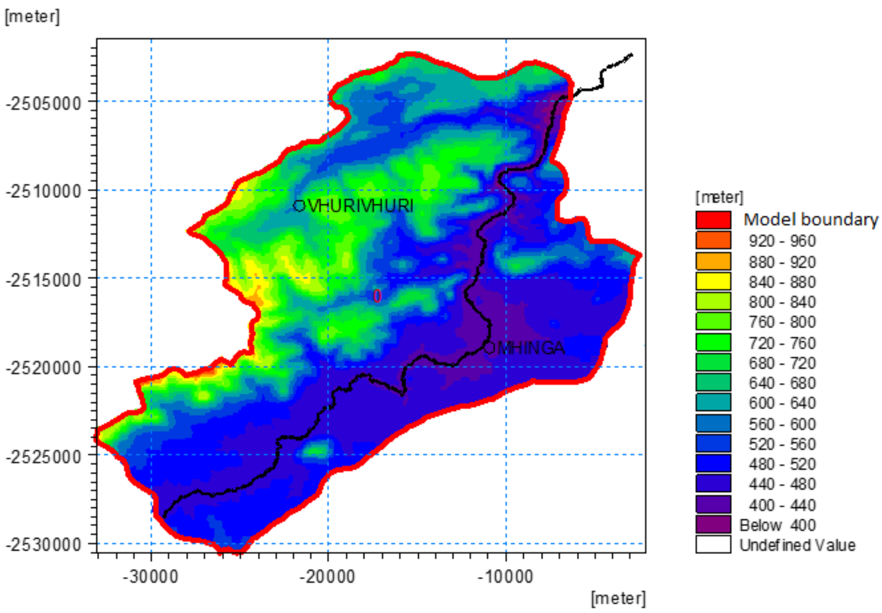


**Figure 3.3: Topographical map showing the model domain**

### 3.2.3 MIKE 11 and MIKE SHE model configuration

The water cycle simulated by the integrated model was represented by models for each component (overland, channel, evapotranspiration, saturated zone and unsaturated zone processes). Table 3.2 shows the suitable approximations which were selected for each process in the study.

**Table 3.2: Summary of MIKE SHE process approximations**

| Process | Approximation |
|---|---|
| Overland Flow | Simple sub-catchment method. |
| Streamflow | 1D - Fully Dynamic Wave Approximation of the St. Venant simulated by MIKE 11. |
| Evapotranspiration | Simplified ET for 2-layer water balance model. |
| Unsaturated Zone | 2-layer water balance model. |
| Saturated Zone | 3D Finite Difference application of Darcy's equation. |

- **Unsaturated flow**

A two-layer water balance algorithm was used to approximate the unsaturated flow. The two-layer approach divides the unsaturated zone into two layers, one on top of the other. The top layer starts from the ground surface and ends at the capillary fringe and the bottom layer extends from the end of the capillary fringe (evapotranspiration extinction depth) to the water table. The two-layer approach uses the Green and Ampt method to estimate infiltration to the unsaturated zone. Water percolates into the water table when soil moisture is more than field capacity. The simple two-layer balance was selected in order to minimise computational effort and time.

- **Saturated flow**

Saturated flow was simulated using finite difference technique of solving Darcy's 3D equation. In the initial simulations, the lumped linear reservoir method was used due to its minimal computational and time requirements. The method highly simplifies the groundwater system by taking the saturated zone as a lumped up model instead of taking it as physically based and fully distributed. This allowed many simulations to be done for testing the model, debugging and dealing with instabilities in reasonable time**.**

- **Overland flow**

The overland runoff is produced after precipitation rate exceeds infiltration rate. Overland runoff was approximated using the sub-catchment method. This lumped approach method is simple and involves the division of the model domain into smaller catchments. The reason for selection was that the approach can be used in high slope areas, for instance, the southern and western parts of the A91H quaternary catchment are mountainous with slope degrees reaching $26^o$. The 2D diffusive wave distributed approach cannot apply to areas where the slope is greater than $15^o$. An empirical relationship between the depth of flow, Manning equation and surface detention is used for routing to streamflow of MIKE 11.

- **Streamflow**

MIKE 11 model was used to approximate streamflow in A91H catchment. In MIKE 11, the Dynamic Wave resolution of Saint Venant equations was used. This formulation together with 3D saturated flow approximation allowed groundwater discharge to be calculated based on water elevation, groundwater head and the river bed conductance term.

The upstream boundary was defined as an open, inflow boundary using the sum of stream flow of stream gauges A9H030 and A9H025. The downstream boundary was defined by an open discharge-water level relation or rating curve (Q-h relationship) (Figure 3.4). The Q-h table was auto-calculated using the critical flow method. Default hydrodynamic (HD) parameters values were used.

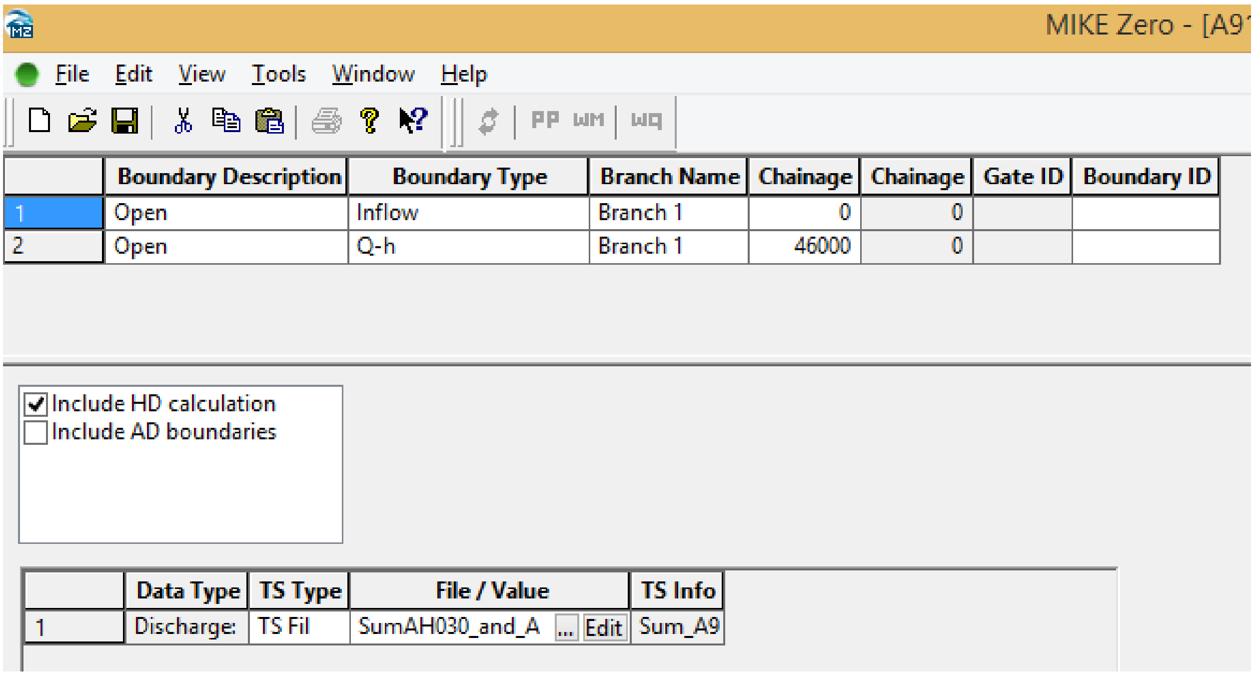


**Figure 3.4: Defined boundary conditions for MIKE 11 model**

- **Evapotranspiration**

The 2-layer evapotranspiration method was used to simulate evapotranspiration. The method is used in conjunction with the 2-layer water balance model for the unsaturated zone. The coupling is an alternative to the more complex unsaturated flow process using Richard's equation coupled to the Kristensen and Jensen model for evapotranspiration. While Richard's equation requires a detailed vertical discretisation of the soil profile (unsaturated zone), the simplified 2-layer method considers the entire unsaturated zone to consist of two layers representing average conditions in the unsaturated zone. The simplified ET for the Two- Layer Water Balance Method uses the formulation in Yan and Smith (1994). The main purpose of the module is to calculate actual evapotranspiration and the amount of water that recharges the saturated zone. The evapotranspiration term includes processes which reduce net rainfall.

Reference evapotranspiration (ETo) was estimated from the climatic data using the Food and Agriculture Organization (FAO) ETo equation 3.1 according to Penman-Monteith methodology (Jensen and Haise, 1963).

$$ET_o = ET_{wind} + ET_{rad} \qquad (3.1)$$

Where $ET_{wind}$ is the wind term, mm/d and $ET_{rad}$ is the radiation term, mm/d.

$$ET_{wind} = PT \times TT\ (e_s - e_a) \tag{3.2}$$

where PT is the term for auxiliary calculation of wind, TT is the temperature term, $e_a$ is the actual vapour pressure, kPa and $e_s$ is the mean saturation vapour pressure derived from air temperature, kPa.

$$ET_{rad} = DT \times R_{ng} \tag{3.3}$$

where DT is the Delta term and $R_{ng}$ is net radiation, mm.

With the 2 - layer method, recharge to the saturated zone (QR) is when the average water content ($\theta_{act}$) exceeds the maximum water content ($\theta_{max}$).

$$QR = \max\ ((\theta_{act} - \theta_{max}\ (z_d)) \cdot z_d, 0) \tag{3.4}$$

- **Coupling the MIKE 11 and MIKE SHE models**

Dynamic coupling of the MIKE 11 and MIKE SHE models was done using the method outlined in DHI (2012). The method allows MIKE 11 model to exchange data with MIKE SHE in a two-way relationship after every computational time step. The dynamic coupling makes use of line segments (river links) on MIKE 11, being placed between adjacent grid squares in MIKE SHE (Figure 3.5). River links are only generated for the area inside the model domain and data exchange only occurs where the river links meet with the MIKE SHE grid squares.

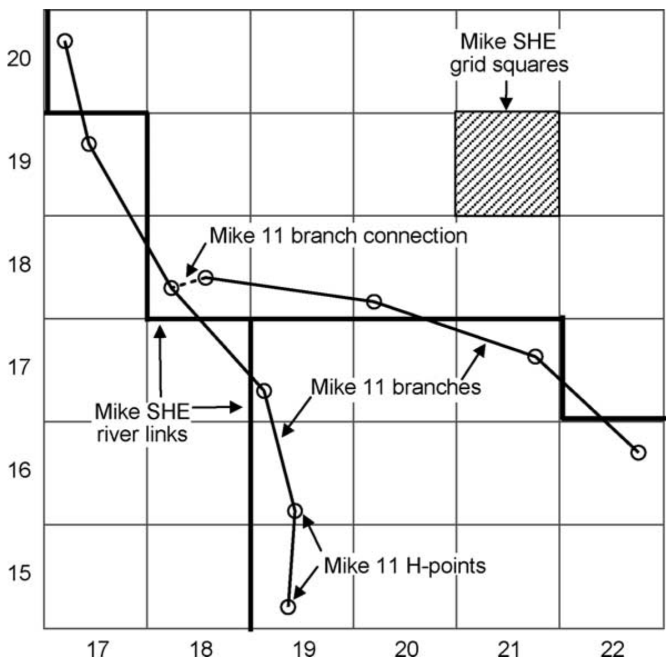


**Figure 3.5: Components of the fully dynamic coupling of MIKE 11 and MIKE SHE model (DHI, 2012).**

Water levels from the MIKE 11 H-points are transferred to adjacent river links. On the other hand, MIKE SHE calculates and transfers overland flow from each grid square to the river links and finally to the H-points. This makes a two-way exchange of data after every time step.

### 3.2.4 Model calibration and validation

MIKE SHE saturated zone model was manually calibrated using the trial and error method. The method involved carrying out many manual calibration simulations until reasonable lower and upper limits of calibration parameters were obtained. Automatic calibration was not considered because it has been found not useful in modelling complex water balances (Kunstmann *et al*. 2006). In the calibration, groundwater levels and streamflow values were used as calibration objectives. Firstly calibration was carried out in the MIKE 11 model to match the simulated to the observed streamflow. After satisfactory MIKE 11 calibration and coupling with MIKE SHE model, the integrated MIKE SHE and MIKE 11 model was calibrated to match the simulated to the observed groundwater levels.

Initial parameter values were either default values from the model, hydraulic parameters from pumping tests or from literature (Thompson *et al*., 2004; Sandu and Virsta, 2015). Sensitivity analysis was carried out to ascertain which parameters affected the model results when they were changed and which ones were insensitive. Sensitivity analysis was done by changing the value of one parameter iteratively while keeping all the other parameters constant. The main calibration parameters were horizontal and vertical hydraulic conductivity ($K_h$ and $K_v$, respectively), specific storage (S), drainage level and drainage time constant.

Although daily streamflow and meteorological data were available from December 1987 to December 2014 and January 1990 to December 2014, respectively, hourly groundwater level data was a limiting factor, since it was only available from December 2004 to December 2014. In addition to this, the groundwater levels data had many gaps. This led to the adjustment of the calibration and validation periods to 1 July 2007 to 31 December 2009 and 1 January 2010 to 21 May 2013, respectively.

### 3.2.5 Evaluating model performance

The model performance was assessed using the standard statistical measures of performance Nash-Sutcliffe coefficient of efficiency (NSE), correlation coefficient (R), root mean square error (RMSE) and mean absolute error (MAE) (Equations 3.5 – 3.8). NSE and R statistics showed the ratio of the scatter or the matching of the simulated values to that of the observed values (Xevi *et al*., 1997). They were used to estimate the correlation between the observed and the simulated groundwater levels. On the other hand, RMSE and MAE were used to estimate the error of the model itself. Root mean square error (RMSE) has been used to measure model performance in environmental studies (McKeen *et al*., 2005). Mean absolute error (MAE) is a useful parameter widely used in model evaluations in general (Jerez *et al*., 2013). The parameters represent different angles of error. Using them in combination has been suggested to be more useful (Chai and Draxler, 2014).

$$NSE = 1 - \frac{\sum(O_i - S_i)}{\sum(O_i - \overline{O_i})} \tag{3.5}$$

$$R = \sqrt{\frac{\sum(S_i - \bar{O}_i)^2}{\sum(O_i - \overline{O_i})^2}} \tag{3.6}$$

$$RMSE = \frac{\sqrt{\sum(O_i - S_i)^2}}{n} \tag{3.7}$$

$$\text{MAE} = \frac{1}{n}\sum|S_i - O_i| \tag{3.8}$$

Where $O$ is observed streamflow ($m^3/s$) or water levels (m), S is simulated streamflow ($m^3/s$) or water levels (m), $\bar{O}$ is the average of observed streamflow or water levels and n is the total number of observations of streamflow or water levels.

### 3.2.6 Groundwater recharge

MIKE SHE model uses the water balance method to estimate groundwater recharge (mm/year) and thus map it. In each pixel, groundwater recharge is calculated using equation 3.9.

(Recharge) $R = P - E_a \pm \Delta W - R_0$ (3.9)

Where $P$ represents precipitation, $E_a$ represents evapotranspiration, $\Delta W$ represents the change in storage for the unsaturated zone and $R_0$ represents surface water discharge.

## 3.3 Groundwater potential assessment

Groundwater potential assessment was done for the A91H quaternary catchment and then downscaled by clipping to the Mhinga area. This was because the study area had limited borehole data for validating the groundwater potential map for Mhinga.

### 3.3.1 Data collection

Remotely sensed data in the form of satellite images, published shape files of geologic faults in South Africa and published faults data were used for groundwater potential assessment. Six 30 m x 30 m resolution images from Landsat Enhanced Thematic Mapper Plus (ETM+) were freely acquired from the United States Geological Services (USGS). The image identities were

LC 81690762013262LGN00, LC 81690762014105LGN00, LC 81690762014153LGN00, LC 81690762014169LGN00, LC 81690762014281LGN00 and LC 81690762015124LGN00. Seven SPOT 5 images with a resolution of 5 m were acquired from South African National Space Agency (SANSA). The image identities were S5 HRG J S5C1 0136 00 0396 00 130228, S5 HRG J S5C1 0136 00 0395 00 130228, S5 HRG B S5C2 0137 00 0395 00 130306, S5 HRG A S5C2 0137 00 0396 00 130306, S5 HRG J S5C2 0137 00 0395 00 150127, S5 HRG T S5C2 0136 00 0395 00 140627 and S5 HRG J S5C2 0136 00 0396 00 140627. Council for Geoscience provided the geological maps and shapefiles.

### 3.3.2 Data analysis: Generation of thematic maps

A total of six thematic maps were prepared based on the factors influencing groundwater potential in the hydrogeological setting of the study area. The themes considered were geologic faults, geology type, rainfall, land use, slope degree and drainage.

Faults thematic map was produced from published geologic faults. The published faults were clipped and verified by physical observation using the SPOT images. Geologic fault zones are usually a good source of groundwater in hard rock terrains. When faulting occurs, the hard rocks fracture and hence fluid conduits and blockages develop on which water can pass and be stored. A double ring buffer was created using ArcGIS 10.2 to map the proximity of an area to the geologic faults. The buffer was used to classify the geologic faults theme into three classes: 0.00 – 250.00 m, 250.01 – 500.00 m and greater than 500.01 m.

Geology shapefile was clipped and reclassified according to the formations which characterise the A91H quaternary catchment. From studies on the geologic formations of the Southpansberg group (Barker, 1983; Du Toit, 1998; Brandl, 1999; Du Toit and Sonnekus, 2010; 2011), groundwater occurrence was related and classified according to geological formations, found in the catchment.

In A91H quaternary catchment, there was no rainfall data. MAP values of weather stations around the quaternary catchment were used, that is, (Punda Maria (0768011A8), Shingwedzi (0768382 0), Letaba (0725373 X), Thohoyandou (0723664 6), Giyani (0724318 9), Levubu (0723485A0) and Kruger (0724790 5) (Figure 3.2). These were interpolated using Inverse Distance Weighting (IDW) method to cover the A91H area. Generally, rainfall is the major contributor to groundwater recharge. Where there is more precipitation, depending on the recharge scheme, more groundwater recharge is expected.

Land use shapefile was obtained from DHI South Africa. The most recent shapefile was selected as a better approximation of the present land use patterns. The land uses were categorized into 13 classes (Figure 3.1). The 13 land use classes were then clustered into four classes: water bodies, settlements, bare land and vegetation to produce the final land use thematic map.

Slope degree map was prepared from a DEM produced using 30 m by 30 m Landsat image. The spatial analyst surface slope feature in the ArcGIS toolbox was used to produce the slope degree thematic map. Flat areas tend to allow water to infiltrate and thus recharge the underground when compared to high slope areas where there is more overland runoff compared to infiltration.

Map showing proximity to drainage was prepared from the digitised drainage network which was generated from the A91H DEM. A double ring buffer was applied to the stream network to demarcate areas which lied within 75 m from the streams and also between 75.01 m to 150 m from the streams. The rest of the area, which lay more than 150 m away from any stream made the third category.

### 3.3.3 Assigning of normalized and class weights

Assigning of normalized weights of each thematic map/layer and weights of attributes in each layer was done using the Analytic Hierarchy Process (AHP) of Saaty (1980). Weights were assigned to thematic maps because the magnitude of influence on groundwater occurrence is different for each theme. The AHP is a multiple decision-making method, which provides a measure of judgement consistency. It also simplifies preference ratings by using pair-wise comparison. AHP was selected over other multi-attribute value techniques because it includes systematic checks on the consistency of judgements (Chowdhury *et al*., 2009 in Fashae *et al*., 2013). The AHP was applied in three successive steps, which were; pair-wise comparison of thematic importance, matrix normalisation and ranking and consistency check.

All thematic factors were compared on a pair wise basis. Comparison of relative importance between two factors is measured according to Saaty's scale (Table 3.3) which has only three choices, i.e. more important, less important or equally important.

**Table 3.3: Scale of importance (Saaty, 1980)**

| Less important | | | | Equally important | More important | | | |
|---|---|---|---|---|---|---|---|---|
| Extremely | Very strongly | Strongly | Moderately | Equal | Moderately | Strongly | Very strongly | Extremely |
| 0.111 | 0.143 | 0.200 | 0.333 | 1 | 3 | 5 | 7 | 9 |

Note: 2, 4, 6 and 8 are intermediate values denoting compromise.

The matrix in Table 3.3 was normalised, by dividing each number in the column by the sum of the column (Equation 3.10).

$$\bar{a}_{jk} = \frac{a_{jk}}{\sum_{i=1}^{m} a_{jk}} \qquad (3.10)$$

Where $\bar{a}$ is value in the matrix, *j* is column number, *k* is row number, *i* is the theme m is the total number of themes. To produce thematic weights $w_j$, from the normalised values, Equation 3.11 was used. The normalised weights were then ranked in descending order.

$$w_j = \frac{\bar{a}_{jk}}{n} \qquad (3.11)$$

It was important to check the consistency of the pair-wise comparison. Consistency check was done following the procedure by Saaty (1980) where,

$$\text{Consistency ratio (CR)} = \frac{CI}{RI} \qquad (3.12)$$

$$\text{Consistency Index (CI)} = \frac{\lambda_{max} - n}{n-1} \qquad (3.13)$$

Where RI is the random index (Table 3.4).

**Table 3.4: Random Index values for n ≤ 10**

| n | 2 | 3 | 4 | 5 | 6 | 7 | 8 | 9 | 10 |
|---|---|---|---|---|---|---|---|---|---|
| RI | 0 | 0.58 | 0.90 | 1.12 | 1.24 | 1.32 | 1.41 | 1.45 | 1.51 |

A consistency ratio (CR) of 0 indicates perfect consistency of pair-wise comparison. Saaty (1980), suggested that acceptable CR should be less than 0.1 and that where values of CR exceed 0.1, the pair-wise comparison will be too inconsistent and thus unreliable.

Each thematic map was reclassified into classes 1 to 4 depending on their influence on groundwater potential. The studies by Rao and Jugran (2003), Prasad *et al*. (2008), Jha *et al*. (2010), Machiwal *et al*. (2011), Mukherjee *et al*. (2012), and Fashae *et al*. (2013) were used as reference when assigning class weights. The most influential attribute in the theme was placed in class 4. The least influential attribute was placed in class 1, with exception of the faults and drainage thematic maps, in which, class 1 represented an attribute with no influence on groundwater. Intermediate attributes were placed in classes 2 and 3.

### 3.3.4 GIS Integration and groundwater potential map

The weighted maps were overlaid using the raster calculator function in ArcGIS 10.2. A simple model was developed, using the model builder to overlay the thematic maps (Figure 3.6).

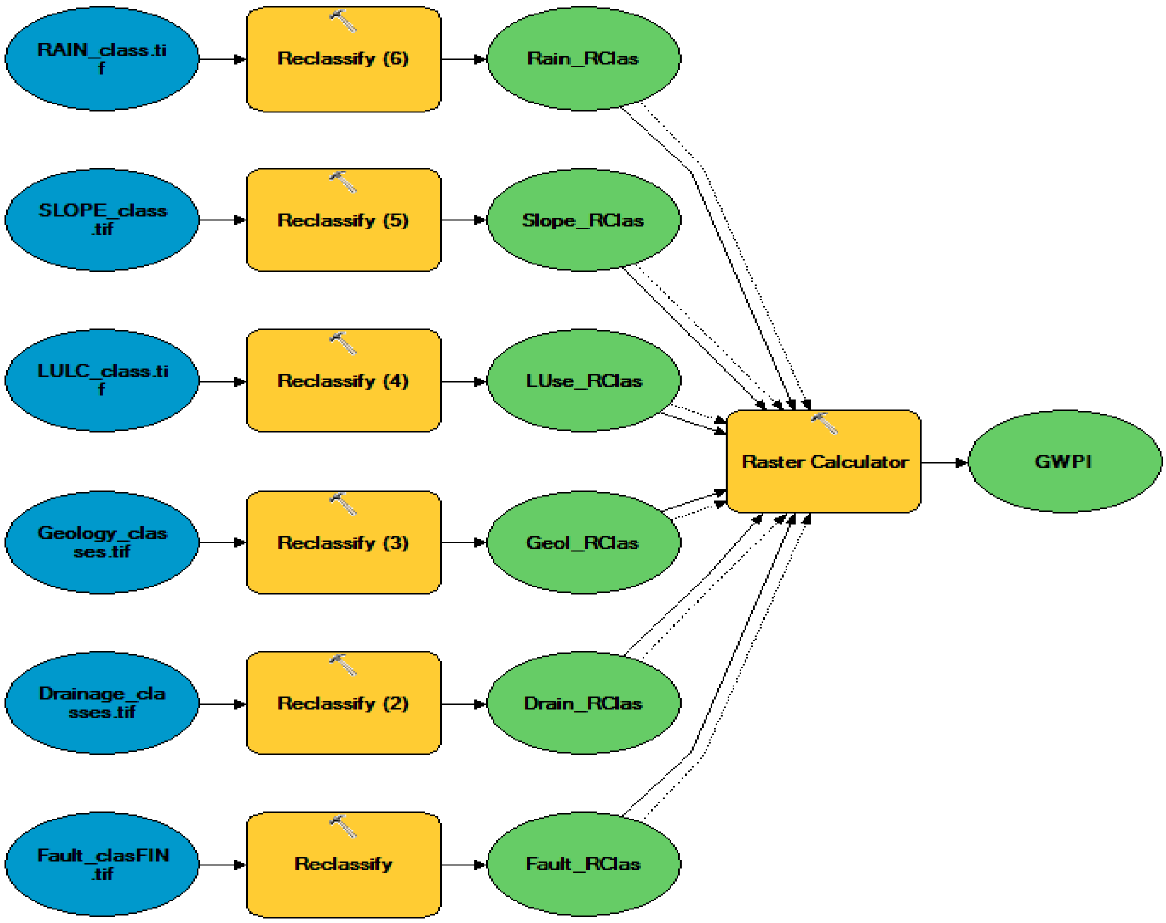


**Figure 3.6: Simple ArcGIS model for the thematic overlay**

In the model, classes inside thematic maps were assigned with weights through the reclassify tool. Subsequently, the new reclassified (RClas) thematic maps were then overlaid using the raster calculator. Groundwater potential was calculated as a groundwater potential index (GWPI) for each cell or pixel (Equation 3.14).

$$GWPI = G_{w_j}G_{w_k} + L_{w_j}L_{w_k} + R_{w_j}R_{w_k} + F_{w_j}F_{w_k} + R_{w_j}R_{w_k} + D_{w_j}D_{w_k} \qquad (3.14)$$

Where F is the proximity to faults, G is geology, R is rainfall, L is land use, S is slope degree, D is proximity to drainage, $w_j$ and $w_k$are as defined earlier.

GWPI was then used to produce the groundwater potential map with four relative classes (very low, low, moderate and high) using the quantile classification method for better visual presentation.

### 3.3.5 Validation of the groundwater potential map

Validation was done by comparing the map produced with the borehole drilling information available. The boreholes drilled in the study area by the municipality were used. The coordinates of the unsuccessful drills were plotted on the groundwater potential map and the corresponding GWP classes they fell in were tabulated. Unsuccessful drills refer to holes drilled which yield less than 0.1 L/s or even no water. The data was analysed to check the frequency and percentage of unsuccessful drills which occurred in each GWP class. Unsuccessful boreholes are most likely to occur in very low GWP zones and least likely to occur in high GWP zones. The validation was such that if there was high frequency of occurrence of unsuccessful boreholes in very low GWP class, then the GWP mapping would be reasonable.

# CHAPTER 4: GROUNDWATER RECHARGE MODELLING

This chapter presents results and discussion of the integrated hydrogeological modelling of Mhinga area. The chapter contains results of coupling MIKE 11 and MIKE SHE models. Also included are the results of pumping tests which were used in the development of a conceptual understanding of the aquifer prior to the groundwater modelling.

## 4.1 Aquifer parameters

Constant discharge rates for the six pumping tests ranged from 0.77 to 5.72 l/s. The estimated transmissivity values ranged from 2.0 to 15.1 $m^2$/day (Table 4.1). Transmissivity and storativity values for the majority of the boreholes were mostly comparable, showing similar groundwater flow and storage behaviour, within the Mhinga aquifer. Borehole H15-0162 had a higher transmissivity than all the boreholes. High transmissivity value implies that more groundwater flows to the borehole in a given time. For example, the high constant discharge rate of 5.72 l/s for H15-0162 is an indication of high transmissivity.

**Table 4.1: Estimated transmissivity and storativity from constant rate pumping tests**

| Borehole | T ($m^2$/day) GRIP project | T ($m^2$/day) Present study | S | Constant discharge rate (l/s) | Duration (Hours) |
|---|---|---|---|---|---|
| H15-0012 | n/a | 2.2 | 0.00042 | 0.85 | 24 |
| H15-0161 | 8 | 2.0 | 0.00038 | 0.77 | 24 |
| H15-0162 | 60 | 15.1 | 0.0028 | 5.72 | 24 |
| H15-0163 | n/a | 2.1 | 0.00040 | 0.81 | 24 |
| H15-0164 | 5 | 2.1 | 0.00040 | 0.81 | 24 |
| H15-0563 | n/a | 2.7 | 0.00050 | 1.02 | 24 |

Some of the pumping test data (Appendix A) were analysed under the Groundwater Resources Information Project (GRIP) dataset using the FC program. The FC program is composed of many different solutions (for example, Theis, Cooper-Jacob, Hantush and Neumann) for estimation of aquifer parameters. In this study, three of the six boreholes' data had been analysed under the GRIP project. The GRIP analyses show that either Theis or Cooper-Jacob were used but it is not clear which one was used to estimate transmissivity. The estimated transmissivities in the GRIP project for borehole H15-0161, H15-0162 and H15-0164 were 8, 60 and 5 $m^2$/day, respectively (Table 4.1). In the present study, the Cooper-Jacob method was used to estimate both transmissivity and storativity. The estimated transmissivity values for this study were all lower than those of the GRIP project. A possible reason for this difference in results from the same boreholes was difference in analytical methods used for analysis. Cooper-Jacob solution is more applicable and highly recommended when using single well data whilst Theis solution is more applicable when observation drawdown data is available. Since the determination of aquifer parameters was not the priority of the GRIP framework all pumping tests were single well tests, with no observation wells. Hence uncertainty in the choice of aquifer analysis solution could have introduced error in the transmissivity values estimated under GRIP. Holland (2011) estimated transmissivity values which ranged from 1 to 330 $m^2$/day, which were higher than the transmissivities obtained in the present study. In his study, he made use of multiple pumping well tests whilst the present study used single well pumping tests. Single pumping well tests are known to produce localised results while multiple pumping well tests produce results for larger area (Kruseman and de Ridder, 2000). Hence, the results in this study were localised which was in line with the small size of the Mhinga area.

Estimated storativity values ranged from 0.00038-0.0028. These mostly fall within the typical range of storativity values for fractured aquifers, which is 0.00001 – 0.001 according to Domenico and Schwartz (1990). Storativity value for H15-0162 is higher than the typical range of storativity values for fractured aquifers (Table 4.1). The high storativity value may be due to a dense network of fractures within the proximity of this borehole, since fractures increase groundwater storage/transmission. Holland (2011) had results of average storativity ranging from 0.007 and 0.05 in the Letaba Lowveld and Limpopo Plateau, respectively, which were comparable to the values found in this study.

## 4.2 MIKE 11 modelling results

NSE values of 0.89 and 0.51 were obtained for MIKE 11 calibration and validation runs, respectively (Table 4.2). R was 0.97 and 0.73 for calibration and validation runs, respectively (Table 4.2). This showed that there was an acceptable fit between the observed and simulated streamflow using MIKE 11 model according to Nash and Sutcliffe (1970) who indicated that NSE > 0.5 shows acceptable fit and Santhi *et al*. (2001) added that R > 0.5 is acceptable. NSE and R, for validation, were low compared to the values for calibration. Possible reasons for this were the shorter length of data used in the validation run, gaps in the validation data set and measurement errors of various input data for the model such as rainfall and groundwater levels. However, according to Moriasi *et al.* (2007), they were acceptable. In the study by Garraway *et al.* (2011) in Mill creek using MIKE 11, computed NSE and R for mean daily streamflow were 0.58 and 0.79, respectively. Andersen *et al*. (2001) had better results with NSE between 0.85 and 0.95. However, they both concluded that reliable data and multi-site calibration (instead of single-site calibration as is in the study) improves model performance.

**Table 4.2: Summary of MIKE 11 model performances**

| **Performance measure** | **Calibration** | **Validation** | **Criteria** |
|---|---|---|---|
| **NSE** | 0.89 | 0.51 | 1 = perfect<br><0.8 good (Nash and Sutcliffe, 1970)<br><0.5 acceptable (Santhi *et al*., 2001) |
| **R** | 0.97 | 0.73 | <0.80 good (Van Liew *et al*., 2003)<br><0.5 acceptable (Van Liew *et al*., 2003) |
| **RMSE** ($m^3/s$) | 3.61 | 7.96 | 0 = Perfect (Moriasi *et al*., 2007)<br><0.5$\sigma$ acceptable (Singh *et al*., 2004) |
| **MAE** ($m^3/s$) | 1.13 | 2.75 | |

Computed RMSE values for the calibration and validation period were 3.61 and 7.96 $m^3/s$, respectively, while MAE values were 1.13 and 2.75 for the calibration and validation periods, respectively. Low and acceptable RMSE and MAE values are those which are less than half of the standard deviation of observed data (Singh *et al*., 2004). Half of standard deviation of the observed calibration data was 5.54. RMSE and MAE were acceptable since they were lower than half of standard deviation. Makungo *et al.* (2010) used MIKE 11 model to simulate rainfall runoff in A80A quaternary catchment, which is located approximately 38 kilometres south-west of A91H quaternary catchment. Computed NSE and RMSE for calibration period were 0.67 and 0.96, respectively. The low NSE was attributed to the existence of data gaps (missing data) in the records and uneven rainfall distribution in the catchment.

RMSE and MAE were greater in the validation period than in the calibration period. Half of the standard deviation of the observed validation data was 9.98 indicating that the errors were within acceptable ranges according to Singh *et al.* (2004).

Graphical fits of observed and simulated streamflow for calibration and validation runs were mostly comparable (Figures 4.1 and 4.2). Simulated streamflow was underestimated forrac all major peaks in the calibration and validation periods. Major peaks occurred after major rainfall events as expected. Underestimations of observed streamflow occurred in October and December 2007, January and March 2008, January, February, March, November and December 2009 (Figure 4.1). In the validation runs, MIKE 11 underestimated observed streamflow between December 2010 and January 2011, December 2012 and February 2013. Underestimation could have been caused by the stream inflow boundary that was set at the upstream boundary of the catchment. The inflow magnitude was the total of the streamflow from station A9H030 and A9H025 (Figure 3.2) and this did not take into account, the streamflow generated from the area between station A9H030 and the upstream boundary of the quaternary catchment or the water losses which are likely to be due to abstractions. Madsen *et al*. (2002) also noted that uncertainties in the measurement of average rainfall and corresponding runoff of the catchment introduce error in the water balance, which then causes underestimation or overestimation by hydrological models. Studies by Makungo *et al.* (2010) and Odiyo *et al.* (2012) also showed that MIKE 11 was not able to simulate peak flows accurately because hydrological phenomena, which occur during high streamflow periods are too complex for rainfall-runoff models due to their inherent structure.

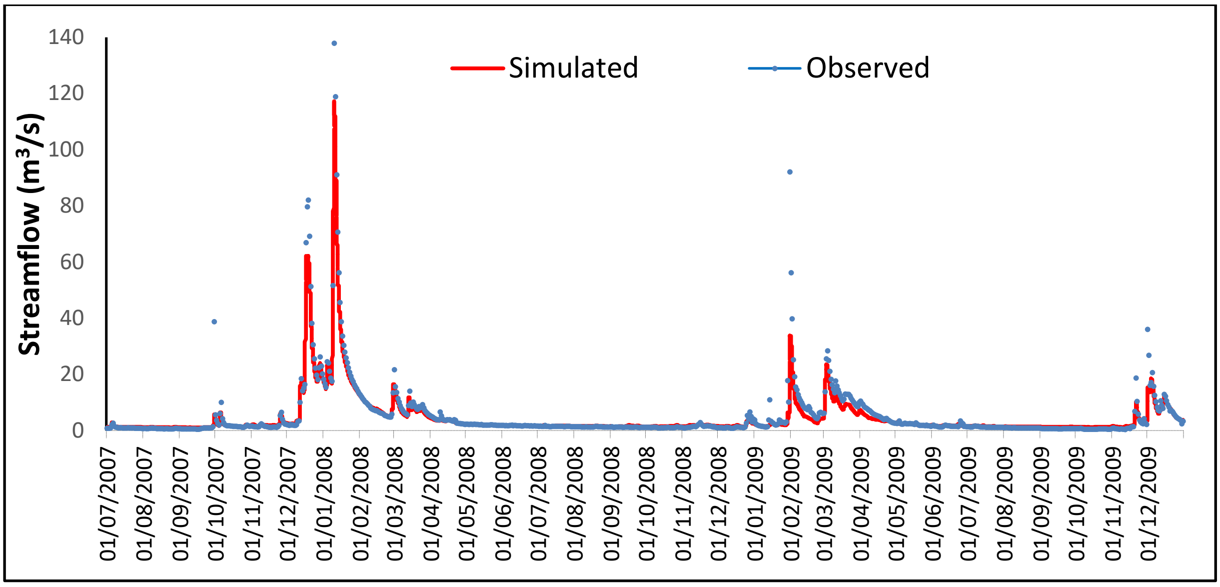


**Figure 4.1: Observed and simulated streamflow in MIKE 11 during calibration period June 2007 to December 2009**

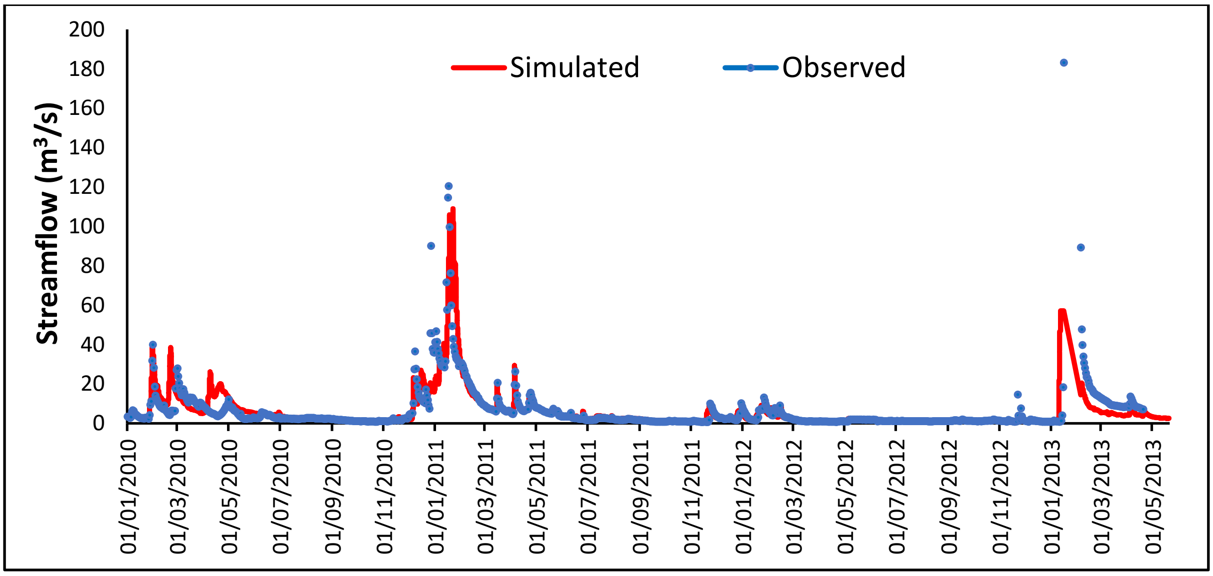


**Figure 4.2: Observed and simulated streamflow in MIKE 11 during validation period January 2010 to May 2013**

However, low flows were well simulated in both calibration and validation runs. Examples of periods where low flows were well simulated include April 2008 to January 2009 and May 2011 to November 2012, in calibration and validation runs, respectively. MIKE 11 successfully modelled the streamflow on Luvuvhu River at Mhinga area (Figure 3.2). The results show that the model is suitable to estimate streamflow on the Luvuvhu River in Mhinga area.

## 4.3 MIKE SHE modelling results

### 4.3.1 Final calibration parameters

The most sensitive parameters identified in the saturated zone were horizontal hydraulic conductivity ($K_h$) and drain time constant ($C_{dr}$) (Table 4.3). This was consistent with the other studies such as Sandu and Virsta (2015) and Thompson *et al*. (2004). Calibration of $K_h$ increased the model sensitivity to rainfall events. The final calibrated average $K_h$ value was 6.25 E-7. Sandu and Virsta (2015) had final calibrated $K_h$ of 4.5 E-6 while Thompson *et al.* (2004) had final calibrated $K_h$ of 1.2 E-8.

**Table 4.3: Final MIKE SHE model calibrated parameters**

| Parameters | Unit | Default parameters | Sandu and Virsta (2015) | Thompson *et al*. (2004) | Present study |
|---|---|---|---|---|---|
| $K_h$ | m/s | 1 E-4 | 4.5 E-6 | 1.2 E-8 | 6.25 E-7 |
| Cdr | 1/sec | 0 | 6.0 E-6 | 1.0 E-7 | 4 E-10 |

### 4.3.2 Model calibration and validation results

NSE values for calibration and validation were 0.84 and 0.72, respectively (Table 4.4). The iterative calibration process produced good fit, between the simulated and the observed groundwater levels in Mhinga according to Nash and Sutcliffe (1970). Liu *et al.* (2007) used MIKE SHE to simulate groundwater levels in the arid Tarim catchment in China and the NSE values ranged from 0.80-0.90 for the calibration runs. Although the NSE value for validation was lower compared to the calibration value, it was in a reasonable range according to Thompson *et al*. (2004), whose NSE values ranged from 0.55-0.80. The NSE values obtained in the present study were thus acceptable and also further supported by Andersen *et al*. (2001).

**Table 4.4: Summary of MIKE SHE model performances**

| **Performance measure** | **Calibration** | **Validation** |
|---|---|---|
| **NSE** | 0.84 | 0.72 |
| **R** | 0.93 | 0.87 |
| **RMSE** (m) | 0.18 | 0.32 |
| **MAE** (m) | 0.13 | 0.26 |

Computed R values were 0.93 for the calibration run and 0.87 for the validation run. The values obtained in the current study were comparable with Thompson *et al*. (2004) whose R ranged from 0.84-0.93. The model performance parameter (R) thus indicated a satisfactory simulation of groundwater levels in an independent validation data set. Computed values of RMSE were 0.18 and 0.32 for the calibration and validation runs, respectively. MAE values for calibration and validation runs were 0.13 and 0.26, respectively. The magnitude of errors were significantly smaller than those obtained in the MIKE 11 modelling. RMSE values fell in the range of other studies like Madsen (2003) and Shalini (2006), RMSE ranges were 0.05-1.03 and 1.00-2.40, respectively. Performance measures showed that model performance was satisfactory. Graphical presentation of MIKE SHE model simulation results for the calibration period showed that simulated groundwater levels were mostly underestimated compared to the observed data (Figure 4.3).

Groundwater levels were mostly overestimated in the validation period (Figure 4.4). In some cases, like February 2013 to May 2013, the magnitude of overestimation was 0.5 m. The observation data was rife with gaps and discontinuities. The major gap was for the period from July 2010 to July 2011. As indicated by Shamsudin and Hashim (2002), gaps in observation data affect the calibration process in a hydrological model. Thus, the overestimations and underestimations could possibly be due to the effect of data gaps and discontinuities.

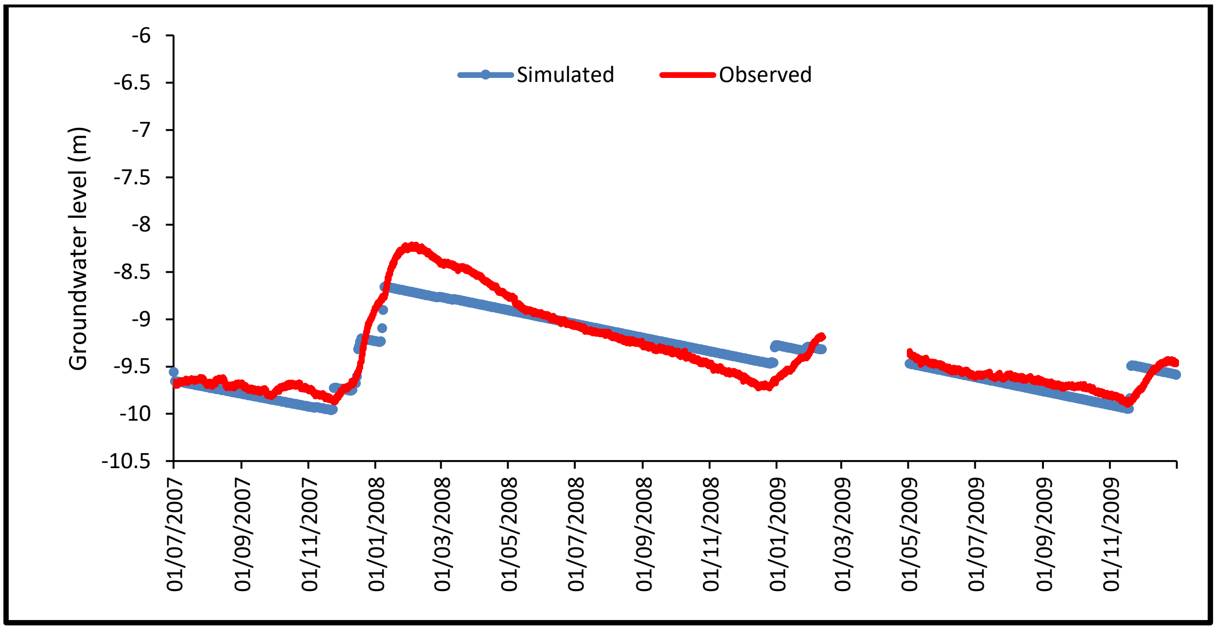


**Figure 4.3: Observed and simulated groundwater levels in MIKE SHE during calibration period June 2007 to December 2009**

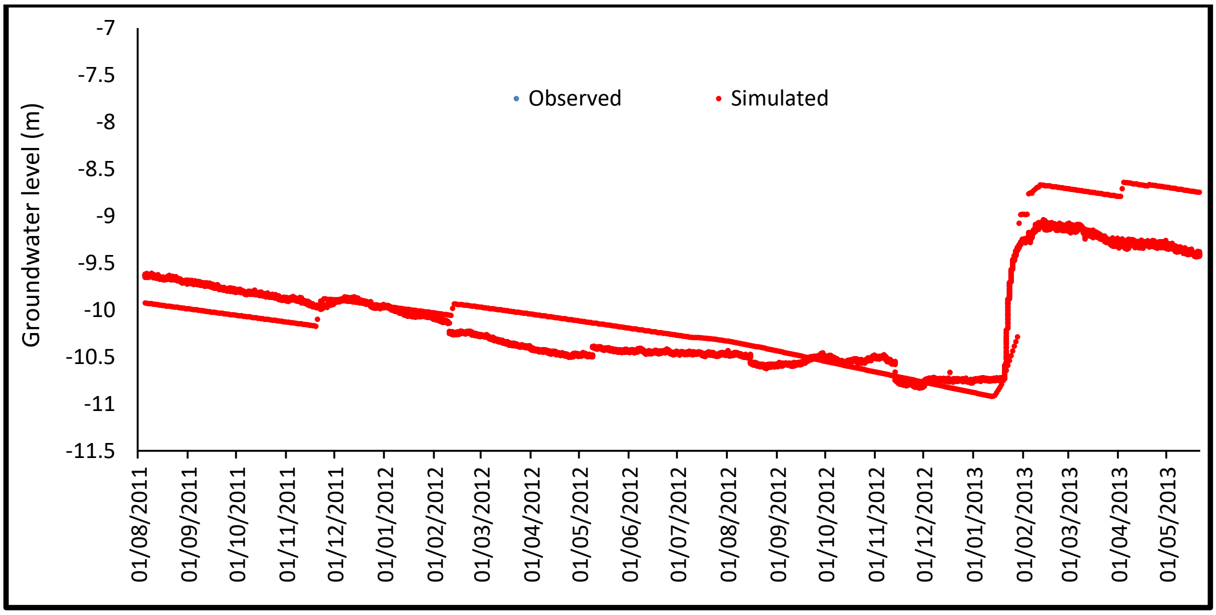


**Figure 4.4: Observed and simulated groundwater levels in MIKE SHE model during validation period January 2010 to May 2013**

Therefore, the MIKE SHE model for the Mhinga area was generally calibrated and validated successfully. It can also be deduced that the model is suitable for use in integrated surface and sub-surface water modelling in data scarce areas like Mhinga.

## 4.4 Groundwater recharge

MIKE SHE computed recharge (Figure 4.5) ranged from 0.00 – 0.4 mm/year in the Mhinga area. This was associated with high ETo (mean of approx. 4 mm/day) (Appendix B) compared to the low precipitation levels (MAP of 656 mm/year). Moreover, Observed groundwater levels were sharply responsive to rainfall events (Appendix C), suggesting a quick response of groundwater levels to rainfall. In the rest of the low slope areas, low recharge was observed.

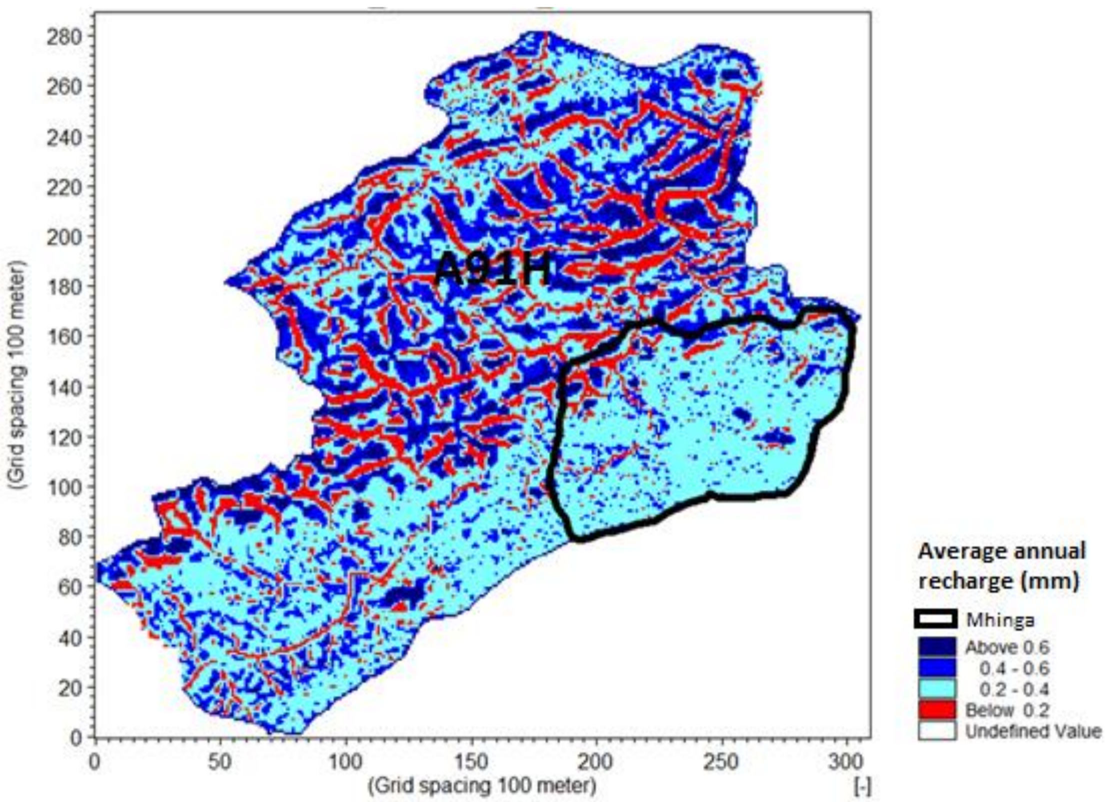


**Figure 4.5: Average annual recharge map**

The annual recharge map (Figure 4.5) also show that the northern parts received higher groundwater recharge than the southern parts. Through comparison of the topographical map (Figure 3.3) and the recharge map, high recharge was observed in the valleys and the lowest recharge on the mountains. This shows that, after precipitation, surface runoff was generated and most of it found its way to the lowest elevation through gravity. The fact that runoff was generated from little precipitation shows that infiltration was low.

The recharge estimates from MIKE SHE were comparable to those obtained in several studies. Holland (2011) in his study around the Letaba Lowveld and Limpopo Plateau, which are located in the same primary catchment with A91H estimated recharge from Chlorine Mass Balance (CMB) and Cumulative Rainfall Departure (CRD) methods. Recharge estimates using CMB ranged from 2.6 – 30.1 mm/year (0.4 – 4.6% of MAP). Using CRD recharge estimates ranged between 11.8 – 16.4 mm/year (1.8 – 2.5% of MAP). The Limpopo River Basin coarse groundwater recharge estimates for the A91H quaternary catchment were 2 to 20.3 mm/year (0.30 – 3.05% of MAP) (WHYMAP, 2008).

However, in a study done in Siloam Village within Nzhelele River by Arrey (2015), on estimating groundwater recharge using a 1-D Hydrus model to simulate groundwater flow from the vadose zone, recharge estimates were higher, between 14.75 and 139.67 mm/year (3.69 and 34.92%). Nemaxwi (2016) had higher estimates of recharge using both the CMB and EARTH model methods in the same area of this study. Estimated recharge rates using CMB were between 0.24 and 78.7 mm/year (0.04 – 12.00% of MAP) for A91H. Using EARTH model, recharge rates ranging from 19.68 to 67.57 mm/year (3.00 – 10.30%) were obtained. A possible reason for the difference in the results with those of the present study may be the use of different simulation models. MIKE SHE model was applied in the saturated zone while the EARTH model was applied to the soil moisture fluctuations in the unsaturated zone.  MIKE SHE model used in the current study makes use of different modules to simulate the overland, channel, evapotranspiration, saturated zone and unsaturated zone processes than the EARTH model used by Nemaxwi (2016). MIKE SHE is a more physically based and distributed model as compared to EARTH model which was used by Nemaxwi (2016).

# CHAPTER 5: GROUNDWATER POTENTIAL ASSESSMENT

## 5.0 Preamble

This chapter presents the results of the application of remote sensing and GIS methods in delineating groundwater potential zones in Mhinga area. Thematic maps, which were produced for each factor considered to influence groundwater potential are presented here. Also presented are the results of the AHP process used to assign weights of themes and the final overlay groundwater potential. Furthermore, discussions relevant to the above-mentioned results are presented.

## 5.1 Results of AHP assigning of weights

Geology was found to be the most important theme when compared to all the themes used in the study. Geology had most importance in all pair-wise comparison (Table 5.1). Proximity to drainage and water bodies such as rivers and lakes was the least important factor. The findings were consistent with those of Fashae *et al*. (2013). Rainfall theme, however, was of second least importance in this study, whereas in the Fashae *et al*. (2013), it had the second most importance. Although rainfall is the major driver of groundwater recharge and potential groundwater availability, there is less spatial variation in Mhinga area with a maximum difference of 140 mm between the highest and lowest rainfall. This means that there is less difference in rainfall amounts between the classes and hence the influence of rainfall on groundwater potential would be more or less the same throughout the area. Saaty's (1980) pair-wise comparison of themes mentioned in Table 3.3 produced Table 5.1, which shows the importance of the themes in the first column relative to the themes on the first row.

**Table 5.1: Matrix showing pair – wise comparison of importance**

| THEME | Geology | Land Use | Slope | Faults | Rainfall | Water Body |
|---|---|---|---|---|---|---|
| **Geology** | **1** | 1 | 1 | 3 | 4 | 5 |
| **Land Use** | 1 | **1** | 1 | 2 | 3 | 4 |
| **Slope** | 1 | 1 | **1** | 2 | 3 | 4 |
| **Faults** | 0.33 | 0.5 | 0.5 | **1** | 2 | 3 |
| **Rainfall** | 0.25 | 0.25 | 0.33 | 0.5 | **1** | 2 |
| **Water Body** | 0.20 | 0.25 | 0.25 | 0.33 | 0.50 | **1** |

According to Saaty (1980), the pair-wise comparison matrix was normalized by dividing each value by the column total and subsequently averaging the row total (Table 5.2).

**Table 5.2: Normalized matrix**

| | Geology | Land Use | Slope | Faults | Rainfall | Water Body | Total | Average/ Normalised | Consistency measure |
|---|---|---|---|---|---|---|---|---|---|
| Geology | 0.26 | 0.25 | 0.24 | 0.34 | 0.30 | 0.26 | 1.66 | 0.28 | 5.26 |
| Land Use | 0.26 | 0.25 | 0.24 | 0.23 | 0.22 | 0.21 | 1.42 | 0.24 | 5.93 |
| Slope | 0.26 | 0.25 | 0.24 | 0.23 | 0.22 | 0.21 | 1.42 | 0.24 | 5.72 |
| Faults | 0.09 | 0.13 | 0.12 | 0.11 | 0.15 | 0.16 | 0.75 | 0.13 | 10.34 |
| Rainfall | 0.07 | 0.06 | 0.08 | 0.06 | 0.07 | 0.11 | 0.45 | 0.07 | 6.97 |
| Water Body | 0.05 | 0.06 | 0.06 | 0.04 | 0.04 | 0.05 | 0.30 | 0.05 | 4.60 |

| | |
|---|---|
| **Λmax** | **6.47** |
| **N** | **6.00** |
| **CI** | **0.09** |
| **RI** | **1.24** |
| **CR=CI/RI** | **0.08** |

**Consistency check**

Computed CR was 0.08 (Table 5.2). CR of 0 shows perfect consistency whereas CR of less than 0.10 is acceptable for weights to be considered as consistent. If CR is greater than 0.10 re-evaluation is recommended to improve the consistency of weights. Fashae *et al.* (2013)

computed CR of 0.02 in weight allocation for eight thematic maps, while CR for Pinto *et al.* (2015) was 0.07. Computed CR for the present study was comparable with other studies and within the acceptable range of less than 0.10. This meant that the assigning of weights was consistent.

## 5.2 Thematic maps

Final computed theme weights, percentage of influence and class weights are shown in Table 5.3. The most influential themes were geology, land use and slope, with thematic weights of 0.28, 0.24 and 0.24, respectively. These three themes altogether had 76% of the influence on groundwater potential.

**Table 5.3: Final weights and ranks**

| Category | Class | Class weight ($W_k$) | Theme weight ($W_j$) | % of influence |
|---|---|---|---|---|
| **Proximity to faults** | | | 0.12 | 12 |
| 0-250 | 3 | 0.50 | | |
| 250.001-500 | 2 | 0.30 | | |
| >500.001 | 1 | 0.20 | | |
| **Geology** | | | 0.28 | 28 |
| Sibasa | 1 | 0.32 | | |
| Wylliespoort | 2 | 0.27 | | |
| Fundudzi | 3 | 0.23 | | |
| Basic Intrusive Rocks | 4 | 0.18 | | |
| **Rainfall** | | | 0.07 | 7 |
| 540 - 580 | 1 | 0.18 | | |
| 580 - 610 | 2 | 0.23 | | |
| 610 - 640 | 3 | 0.27 | | |
| 640 - 680 | 4 | 0.32 | | |
| **Land use** | | | 0.24 | 24 |
| water bodies | 0 | 0 | | |
| Settlements | 1 | 0.21 | | |
| Bare land | 2 | 0.31 | | |
| Vegetation | 3 | 0.48 | | |
| **Slope** | | | 0.24 | 24 |
| 0 - 4.000 | 4 | 0.32 | | |
| 4.001 - 8.000 | 3 | 0.28 | | |
| 8.001 - 12.000 | 2 | 0.22 | | |
| > 12.001 | 1 | 0.18 | | |
| **Proximity to drainage** | | | 0.05 | 5 |
| 0 - 75 | 3 | 0.50 | | |
| 75 - 150 | 2 | 0.30 | | |
| > 150 | 1 | 0.20 | | |

## Geology

Geology had the highest thematic weight of 0.28. Krishnamurthy and Srinivas (1995) pointed out the importance of geology in groundwater potential mapping. The A91H quaternary catchment is located in the Soutpansberg Group which has fractured and intergranular aquifers. There were four formations identified in the quaternary catchment (Wyllie's Poort, Fundudzi, Sibasa and Basic intrusive rock formations).

The Wyllie's Poort Formation (Figure 5.1), is dominated by red-pink quartzite with minor pebble washes and the base of the Formation is marked by a prominent agate pebble conglomerate (Bumby *et al*., 2002). The Formation predominantly covered the quaternary catchment (49.5%). The Fundudzi Formation consists generally of sandstone with a few thin pyroclastic beds (Bumby *et al*., 2002) with intercalated basaltic lava at the top of the succession occupying 68.94 km$^2$ (37.6%) of the total area. The Sibasa Formation is dominated by massive volcanic rocks, that are basaltic in composition, with intercalated pyroclastic and sandstone lenses (Bumby *et al*., 2002) and occupies 45.66 km$^2$ (10.2%) of the total area. The basic intrusive rocks formation had the least coverage of the quaternary catchment of just 12.82 km$^2$ (2.9%).

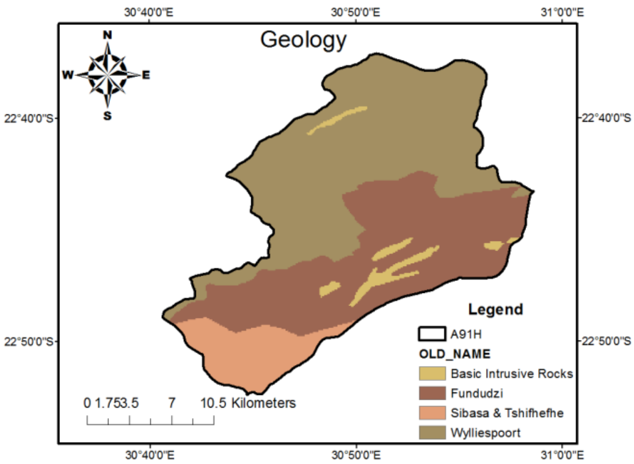


**Figure 5.1: Geology**

The geohydrology studies by Du Toit (1998); Du Toit and Sonnekus (2010) and Lourens (2013) classified the Soutpansberg formations according to aquifer potential. Sibasa, Wyllie's Poort and Fundudzi Formations had moderate low, low and very low aquifer potential, respectively. Thus, the normalized weights were assigned in that order, with 0.32, 0.27 and 0.23, 0.18 for Sibasa, Wyllie's Poort, Fundudzi and Basic intrusive rock formations, respectively.

## Land use

The consolidation of the 13 land uses produced four land use types (Figure 5.2). Water bodies comprised of seasonal water and permanent water/wetland aggregating a small total area of 1.53 km$^2$ (0.34%). Vegetation comprised of indigenous forest, thicket, woodland, grassland, cultivated commercial fields, orchards and plantations covering the major part of 372.72 km$^2$ (83.30%) of the quaternary catchment. Bare soil covered only 0.49 km$^2$ (0.11%) while settlements included cultivated subsistence, mines, urban village and built up areas covering 72.97 km$^2$ (16.22%). Water bodies were assigned a normalized weight of 0 because they were not considered as borehole drilling targets. Vegetation had the highest weighting of 0.48 (Table 5.3) because vegetation grows where there is water and where agriculture is being practised and usually irrigation recharges the aquifer. Bare land was assigned a weight of 0.31 and settlements were assigned weighting of 0.21 mainly due to the impervious nature of the ground surfaces in these land use types.

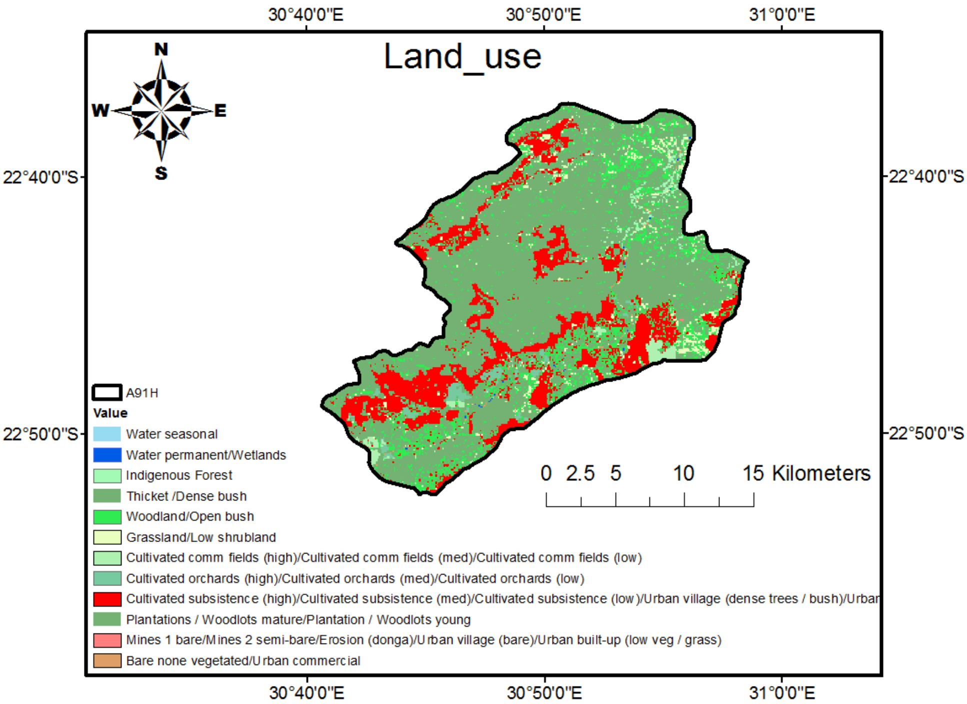


**Figure 5.2: Land use**

### Slope

Slope degree had a computed weight of 0.24. Jasmin and Mallikarjuna (2011) listed slope degree as a salient feature in groundwater potential mapping. Slope from 0.00° to 4.00° was assigned the highest normalized weight of 0.32, whereas the areas with the slope degree (over 12°) were assigned the lowest weight of 0.18 (Figure 5.3). Areas with low slope degree allow more water to infiltrate than to runoff on the surface. From the south western to the eastern border of the quaternary catchment, the slope was low (0 – 4°) while the rest of the quaternary catchment was high (greater than 4°). Majority of the quaternary catchment area of 294.55 $km^2$ (65.47%) had low slope of 0 - 4.00° and 103.43 $km^2$ (22.99%) had 4.00 - 8.00°. Area coverage for the class 8.00 – 12.00° was 36.49 $km^2$ (8.11%) and for slope greater than 12.00°, was 15.39 (3.42%).

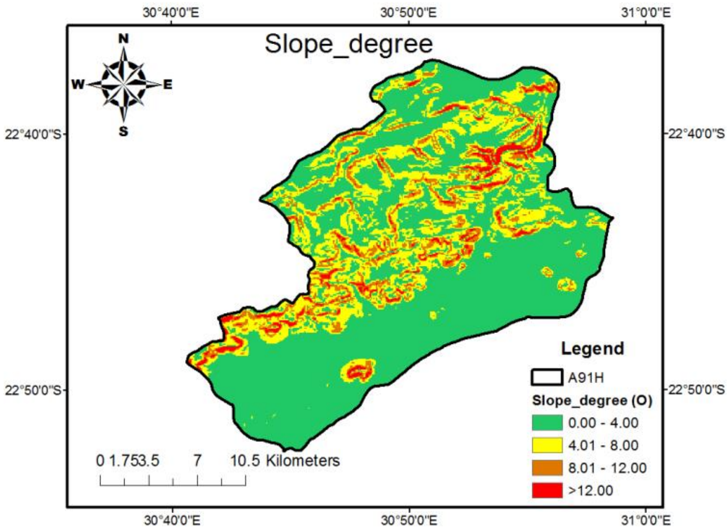


**Figure 5.3: Slope degree**

### Rainfall

Interpolated Mean Annual Precipitation (MAP) ranged from 540 mm to 680 mm (Figure 5.4). Generally, rainfall is the major contributor to groundwater recharge. Where there is more precipitation, depending on the recharge scheme, more groundwater recharge is expected. The weight assigned to the rainfall theme was 0.074 (Table 5.3). The weight was significantly lower than what was computed in other studies. For example, in Al Saud (2010), rainfall was the most influential and had the weight of 0.30 while in Senanayake *et al*. (2016), the weight was 0.15

and in Fashae *et al*. (2013), rainfall weight was 0.17. This deviation was due to the differences in the variation of MAP in the studies. In the current study, rainfall varied from 541 – 680 mm/year, which is too low in terms of influence on groundwater potential zones. Conversely, in Fashae *et al.* (2013), mean annual rainfall varied from 1 164 – 1 776 mm/year, which was considerable to ascertain that difference in MAP could influence groundwater potential. This was an advantage of using the Saaty's AHP process of assigning weights as it gives room to make pair-wise comparison which is relevant for the scenarios.

Normalized weights of 0.32, 0.27, 0.23 and 0.18 (Table 5.3) were assigned to MAP of 640 mm – 680 mm, 610 mm – 640 mm, 580 mm – 610 mm ad 540 mm – 580 mm, respectively. 49.89 km$^2$ (11.09%) and 153.37 km$^2$ (34.09%) of the quaternary catchment had interpolated MAP of 540 – 580 mm and 580 – 610 mm, respectively. Most of the area, 189.99km$^2$ (42.23%) was covered by rainfall in the range of 610 – 640 mm and 56.60 km$^2$ (12.58%) was covered by the highest rainfall in the quaternary catchment ranging from 640 – 680 mm.

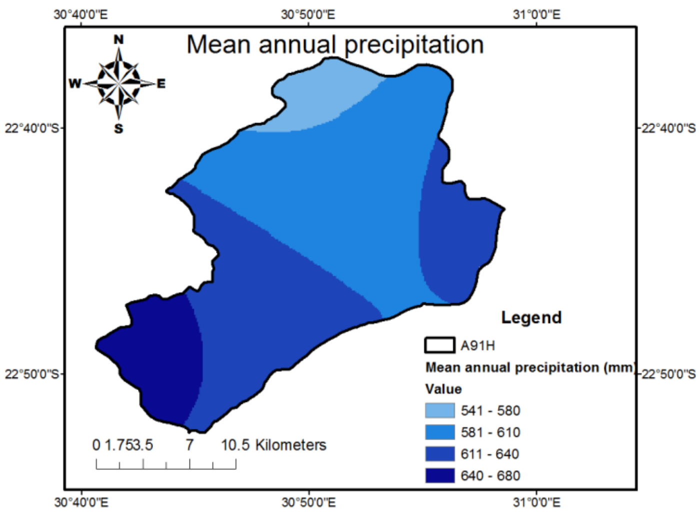


**Figure 5.4: Rainfall**

**Distance to faults**

The computed thematic weight of the distance to faults was 0.12 (Table 5.3). The weight shows that the theme had a small influence on groundwater potential. Sreela *et al*. (2013) regarded geologic faults as the most influencing factor. However, Fashae *et al*. (2013) assigned the theme with a weight of 0.08, which was low and comparable to the findings of this study. This was similar to the conclusion by Jasmin and Mallikarjuna (2011) in their review of studies using RS and GIS to map groundwater potential areas. The buffer applied produced three classes: 0.00 m – 250.00 m, 250.01 m – 500.00 m and greater than 500.01 m with normalised weights: 0.50, 0.30 and 0.20, respectively (Figure 5.5). 87.6 $km^2$ (19.48%) of the quaternary catchment was within 250 m of a geologic fault while 74.23 $km^2$ (16.5%) was between 250 and 500 m from a geologic fault and 287.89 $km^2$ (63.99%) was further than 500 m from a geologic fault. The influence on groundwater potential decreased inversely with the distance from the geologic faults.

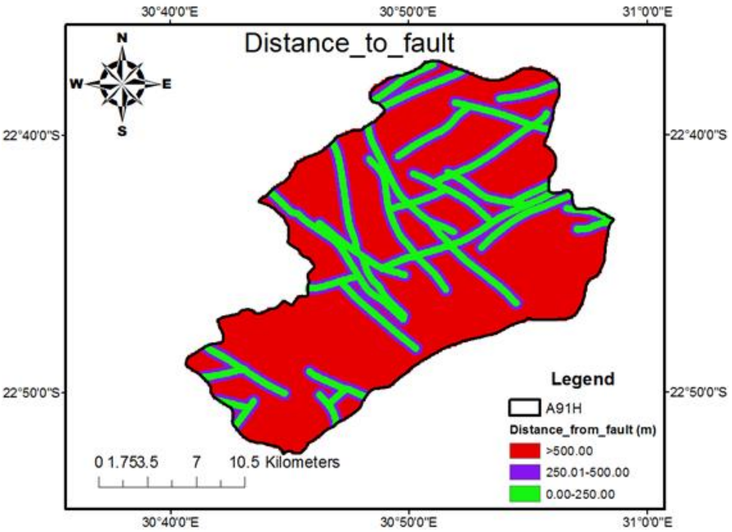


**Figure 5.5: Distance to fault**

**Proximity to drainage**

Three proximity classes (0 -75 m; 75 – 150 m and > 150 m) were produced by the multiple buffer. The highest weights were assigned to the area closest to the drainage network. Close proximity to drainage means that water is more likely to infiltrate laterally and thus recharge the area. Further away from any drainage means that the influence of the drainage reduces. The rate of reduction is high since groundwater is generally considered to move very slowly. Areas between 0 m and 75 m (Figure 5.6) from drainage were assigned a weight of 0.50 followed by areas between 75 m and 150 m from drainage, which were assigned a weight of 0.30 (Table 5.3). Areas located more than 150 m from drainage were allocated weightage of 0.20.

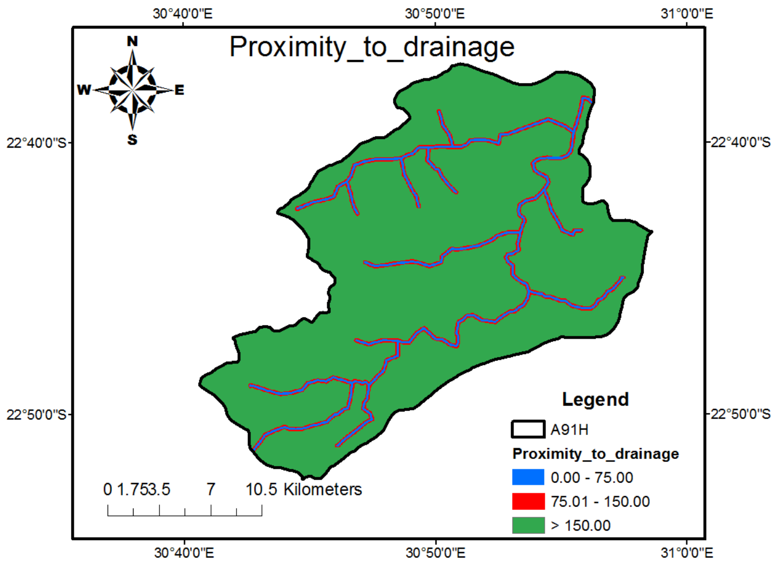


**Figure 5.6: Proximity to drainage**

## 5.3 Groundwater potential map

Groundwater potential ranged from 1.76 to 3.66. Quantile classification produced four distinct zones of groundwater potential, which were 1.76 – 2.81, 2.81 – 2.90, 2.90 – 3.07 and 3.07 – 3.66, representing very low, low, moderate and high classes, respectively (Figure 5.7). High groundwater potential was mainly found in the south western tip of the A91H quaternary catchment. This region was mainly characterised by a combination of the best geology (Sibasa Formation), rainfall (611 – 680 mm) and slope (0.00 – 4.00°), and high occurrence of faults and water bodies in the A91H. Other areas with high groundwater potential were located mainly in the upper hemisphere of the A91H quaternary catchment. A closer look at the thematic maps (Figures 5.1-5.6) reveals that high groundwater potential is associated with proximity to geologic faults of the area. These findings were consistent with Krishnamurthy and Srinivas (1995), who concluded that geology of an area heavily influences groundwater potential.

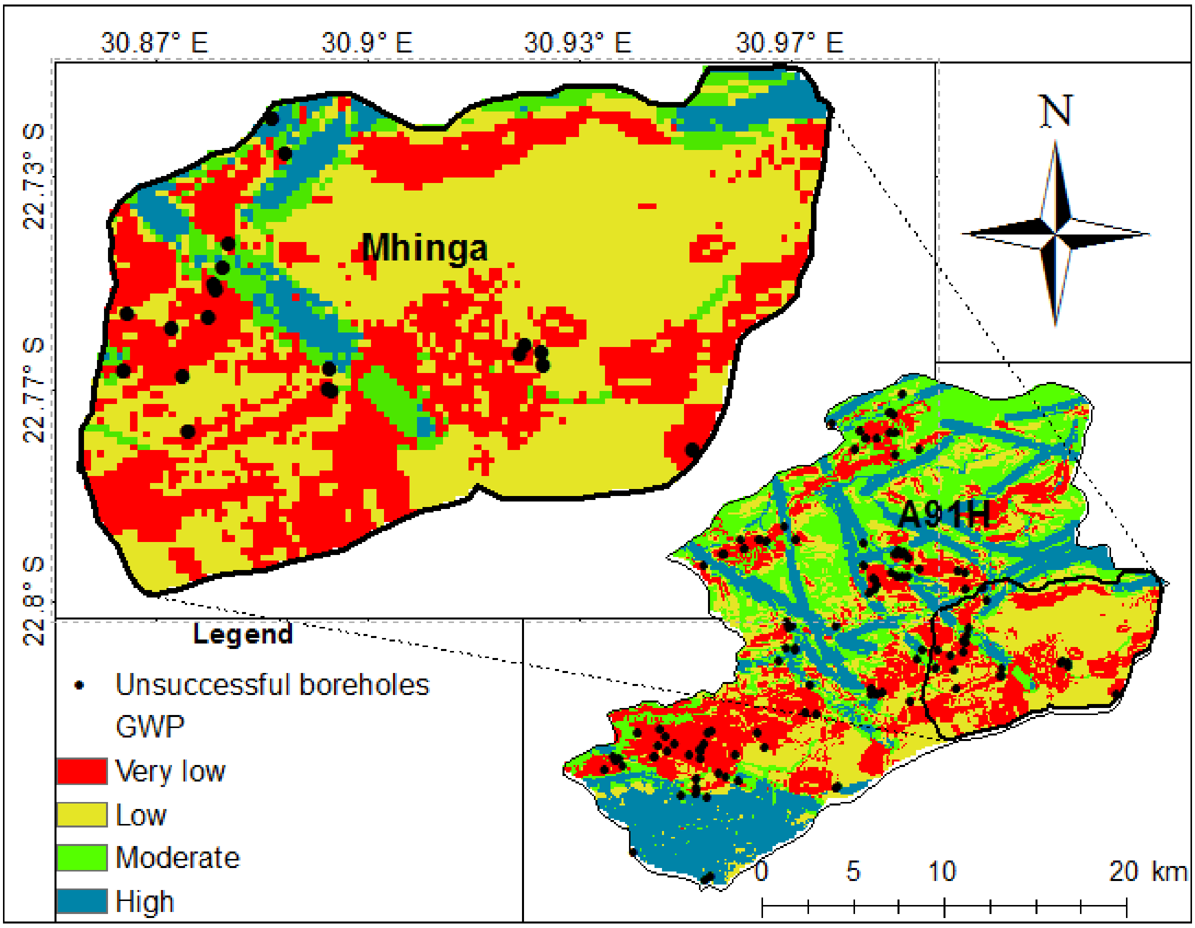


**Figure 5.7: Groundwater potential map of Mhinga area**

The areas with moderate groundwater potential coincided with the locations where the Wylliespoort formation is found. The formation had the highest rank in the geology theme. The low to very low groundwater potential were found in areas within Fundudzi Formation, with human settlements and high slope areas (slope > 8.00°). Due to the high rainfall in the south eastern parts (Figure 5.4), it was expected that groundwater potential would be high, but the opposite of this scenario was observed. Since rainfall had very small theme weight ($w_j$) of 0.07, its influence was overridden by the geology whose thematic weight ($w_j$) was 0.28. This situation then shows the importance of including more than one factor in groundwater potential studies, because the factors affect groundwater potential in an integrated way.

Mhinga area was mainly covered by areas of very low and low groundwater potential. This could have been because most of the area lies on the Fundudzi formation (Figure 5.1), which has low weight in the geology theme. In terms of area coverage, 34.47, 51.39, 7.66 and 6.48%

had very low, low, moderate and high groundwater potential, respectively. In the Mhinga area, moderate to high groundwater potential was solely located in the geologic fault zones.

## 5.4 Validation with borehole data

Borehole drilling statistics of the boreholes in A91H quaternary catchment was used to validate the groundwater potential map. Of the total 112 unsuccessful boreholes drilled, 69 (61.6 %) fell in the very low GWP zones, 16 (14.3 %) fell in the low GWP zones, 17 (15.2 %) fell in moderate GWP zones and 10 (8.9 %) fell in the high GWP zones (Figure 5.8). In the Mhinga area, a total of 19 unsuccessful boreholes were drilled of which, 11 (57.9%) fell in the very low GWP zones, while 6 (31.6%) fell in the low GWP zones and 2 (10.5%) fell in the moderate GWP zone (Figure 5.8).

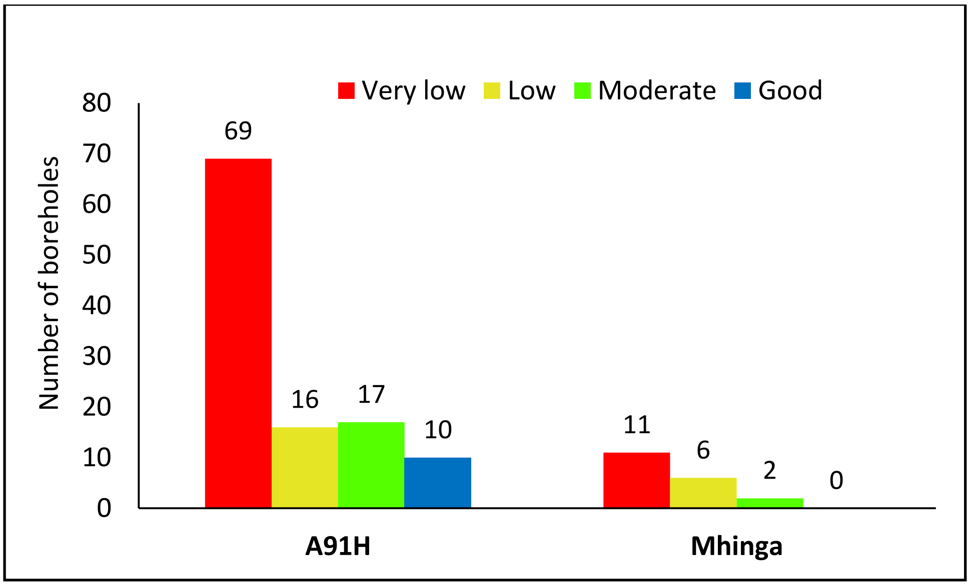


**Figure 5.8: Unsuccessful boreholes drills and corresponding GWP classes**

Hence in Mhinga area, 89.5% of all the unsuccessful boreholes drilled occurred in the very low to low GWP zones. Furthermore, no unsuccessful boreholes drilled were observed in the high GWP zone. The high frequency of unsuccessful drilling in mainly the very low and low GWP classes in both Mhinga area and A91H quaternary catchment, validates the results of this study and show that the GWP zones delineated in the current study are realistic.

# CHAPTER 6: CONCLUSION AND RECOMMENDATIONS

This study was aimed at estimating groundwater recharge and demarcating groundwater potential zones in the Mhinga area. Groundwater recharge was estimated using an integrated MIKE 11 and MIKE SHE model. Calibration and validation of the coupled model were done using data for the periods 01/07/2007 to 31/12/2009 and 01/01/2010 to 21/05/2013, respectively. NSE, R, RMSE and MAE for calibration and validation runs of MIKE 11 model range from 0.51 - 0.89, 0.73 - 0.97, 3.61 - 7.96 and 1.13 - 2.00, respectively. The model underestimated the peak flows after rainfall events. This was likely because the complex nature of high flow events is difficult to simulate using rainfall-runoff models due to their inherent structure. NSE, R, RMSE and MAE for calibration and validation runs of the integrated MIKE 11-MIKE SHE model were 0.72 - 0.84, 0.87 - 0.93, 0.18 - 0.32 and 0.13 - 0.26, respectively. The integrated MIKE 11-MIKE SHE model both underestimated and overestimated observed streamflow and groundwater levels in the calibration and validation runs. This could have been caused by uncertainties in measured input data. Measures of performance and graphical fits showed that the model can reasonably estimate groundwater recharge. In addition, the study also showed that MIKE 11 model was capable of simulating streamflow and that MIKE SHE model was capable of simulating integrated groundwater flow. The estimated recharge ranged from 0 to 2.75 mm/year (0 – 0.42% of MAP) for the A91H quaternary catchment.

An ArcGIS model was developed for overlaying thematic maps of factors which influence groundwater potential. AHP was used to assign weights for faults, geology, rainfall, land use, slope degree and proximity to drainage themes. The most influential themes were geology, land use and slope, respectively. These three themes altogether had 76% of the influence on groundwater potential. Mhinga area was mainly covered by areas with very low and low groundwater potential. In terms of area of coverage, 34.47, 51.39, 7.66 and 6.48% had very low, low, moderate and high groundwater potential, respectively. Validation using borehole drilling data clearly showed the delineated GWP zones were realistic. Thus, the integrated use of AHP, remote sensing and GIS methods in the study were useful for assessing GWP. It is recommended that the integrated model be developed and improved as more data is collected to refine the conceptualisation of the aquifer and accurate determination of groundwater recharge. It is recommended that a designed network of groundwater data collection including monitoring boreholes and a weather station be established in A91H. Borehole logging and long duration pumping tests will also be necessary for new and existing boreholes which are essential for estimation of hydraulic aquifer parameters. It is also recommended that the ArcGIS model produced can be further modified and developed by incorporating finer resolution images and shapefiles.

## References


Aboyeji, O.S., Mogaji, K.A. and Oyinloye, R.O., 2012. Structural interpretation of remotely sensed data sets, its hydrogeological implication over ile-ife and environs. *Ozean Journal of Applied Sciences*, vol. 5(1), pp. 43-54.

Al Saud, M., 2010. Mapping potential areas for groundwater storage in Wadi Aurnah Basin, western Arabian Peninsula, using remote sensing and geographic information system techniques. *Hydrogeology Journal*, vol. 18(6), pp.1481-1495.

Andersen, J., Refsgaard, J.C. and Jensen, K.H., 2001. Distributed hydrological modeling of the Senegal River Basin-model construction and validation. *Journal of Hydrology*, vol. 247, pp. 200-214.

Arrey, I.A., 2015. Estimating groundwater recharge from infiltration in the unsaturated zone, a data integration and modelling approach: Siloam Village case study. M.Sc. Thesis (unpublished), University of Venda, Thohoyandou pp.

Avinash, K., Jayappa, K.S. and Deepika, B., 2011. Prioritisation of sub-basins based on geomorphology and morphometric analysis using remote sensing and geographical information system (GIS) techniques. *Geocarto International*, vol. 26(7), pp. 569–592.

Barker, O.B., 1979. A contribution to the geology of the Soutpansberg group, Waterberg supergroup, northern Transvaal. M.Sc. Thesis (unpublished), University of Witswatersrand, Johannesburg, pp. 116.

Barker, O.B., 1983. A proposed geotectonic model for the Soutpansberg Group within the Limpopo Mobile Belt, South Africa. Special Publication. *Geological Society South Africa*, vol. 8, pp. 181 –190.

Bear, J., 1972. Dynamics of Fluids in Porous Media. *New York*: Dover Publications.

Beekman, H.E., Gieske, A. and Selaolo, E.T., 1996. GRES: Groundwater recharge studies in Botswana 1987-1996. *Botswana Journal of Earth Sciences*, vol. 3, pp. 1-17.

Brandl, G., 1999. Southpansberg Group. In: Johnson, M.R. (Ed), Catalogue of South African lithostratigraphic units. *South African Committee for Stratigraphy*, pp. 6-39.

Bredenkamp, D.B., Botha, L.J., van Tonder, G.J. and van Rensburg, H.J., 1995. Manual on quantitative estimation of groundwater recharge and aquifer storativity. *Water Research Commission. Pretoria*, pp. 407.

Bumby, A.J., Eriksson, P.G., Van der Merwe, R. and Steyn, G.L., 2002. A half-graben setting for the Proterozoic Soutpansberg Group (South Africa): evidence from the Blouberg area. *Sedimentary Geology*, vol. 147(1), pp.37-56.

Camp Dresser and McKee Incorporated, 2001. Evaluation of integrated surface water and groundwater modelling tools. Water resources research & development program. [pdf] Denmark: Danish Hydrology Institute (DHI). Available at: http://www.mikebydhi.com/upload/dhisoftwarearchive/papersanddocs/waterresources/MSHE_Code_Evaluations/CDM_ISGW_Report.pdf [Accessed 11 June 2014]

Chai, T. and Draxler, R.R., 2014. Root mean square error (RMSE) or mean absolute error (MAE) – Arguments against avoiding RMSE in the literature. Geoscientific model development discussion, vol. 7(3), pp. 1247-1250.

Chowdhury, A., Jha, M.K., Chowdary, V.M. and Mal, B.C., 2009. Integrated remote sensing and GIS-based approach for assessing groundwater potential in West Medinipur district, West Bengal, India. *International Journal of Remote Sensing*, vol. 30(1), pp. 231-250.

Cooper, H.H. and Jacob, C.E., 1946. A generalized graphical method for evaluating formation constants and summarizing well field history. *Transactions of the American Geophysical Union*, vol. 27(4), pp. 526-534.

Danish Hydrologic Institute (DHI), 2012. MIKE SHE user manual, vol. 2: Reference guide. DHI Water and Environment, Hørsholm, Denmark.

Department of Water Affairs and Forestry (DWAF), 2004. National water resource strategy. 1st Edition, *Department of Water Affairs and Forestry. Pretoria*, pp. 150.

Department of Water Affairs and Forestry (DWAF), 2006. Groundwater resource assessment ii – task 3 recharge. *Department of Water Affairs and Forestry. Pretoria*.

Domenico, P.A. and Schwartz, F.W., 1990. *Physical and chemical hydrogeology*, John Wiley and sons, New York, pp. 824.

Du Toit, W. H., 1998. Geohidrologie van die Nasionale Krugerwildtuin gebaseer of die evaluering van bestaande boorgatinligting. Report No. GH3806: *Department of Water Affairs and Forestry. Pretoria.*

Du Toit, W. H. and Sonnekus, C., 2010. Explanation of the 1:500 000 Hydrogeological map 2326 Polokwane: *Department of Water Affairs. Pretoria.*

Du Toit, W. H. and Sonnekus, C. J., 2011. Explanatoin of the 1:500 000 Hydrogeological map 2127 Messina: *Department of Water Affairs. Pretoria.*

Du Toit, W., Holland, M., Weidemann, R. and Botha, F., 2012. Can groundwater be successfully implemented as a bulk water resource within rural Limpopo Province? Analysis based on GRIP. *Water SA*, vol. 38(3), pp. 391-397.

Fashae, O.A., Tijani, M.N., Talabi, A.O. and Adedeji, O.I., 2013. Delineation of groundwater potential zones in the crystalline basement terrain of SW-Nigeria: an integrated GIS and remote sensing approach. *Applied Water Science*, vol. 4(1), pp. 19-38.

Foster, S. and Ait-Kadi, M. 2012. Integrated water resources management (IWRM): How does groundwater fit in? *Hydrogeology Journal*, vol. 20(3), pp. 415-418.

Freeze, R.A. and Cherry, J.A., 1979. Groundwater. Prentice Hall Inc., New Jersey, pp. 604.

Garraway, M., Milford, L., Van Vliet, D., Bellamy, S., Murray, S., Gabriel, C., Jones, J.P., Delaney, P. and Qiao, Y. Neville, C., 2011. Integrated surface and groundwater model review and technical guide, AquaResource Inc.

Gieske, A., 1992. Dynamics of Groundwater Recharge - A case study in semi-arid eastern Botswana. PhD Thesis, Free University, Amsterdam, pp. 290.

Gimblett, R., 1989. Innovations in computer labs. Linking perception research, visual simulations and dynamic modeling within a GIS framework: The ball state experience computers. *Environment and Urban Systems*, vol. 13(2), pp. 109–123.

Gordon, S., Jones, J.P., Jackstiet, R. and Diiwu, J., 2005. Review of groundwater and surface water interaction - knowledge and modelling approaches for streamflow prediction in Alberta. Prepared by the Alberta Research Council for Michael Seneka of Alberta Environment.

Hansen, J.R., Refsgaard, J.C., Hansen, S. and Ernstsen V., 2007. Problems with heterogeneity in physically based agricultural catchment models. *Journal of Hydrology*, vol. 342(1-2), pp. 1-16.

Harbaugh, A.W., 2005. MODFLOW-2005, the U.S. Geological Survey modular groundwater model. United States Geological Survey Techniques and Methods 6-A16.

Hill, J.M., Harlow, C.A. and Zimmerman, P., 1983. Geographic information systems as applied to the manipulation of environmental data. *The Environmentalist*, vol. 3(1), pp. 33–38.

Hiscock, K., 2005. Hydrogeology. Principles and practice. Carlton: Blackwell Publishing. ISBN: 978-0-632-05763-4, pp.544.

Hoffmann, J. and Sander, P., 2007. Remote sensing and GIS in hydrogeology. *Hydrogeology Journal*, vol. 15(1), pp. 1–3

Holland, M. 2011. Hydrogeological characterisation of crystalline basement aquifers within the Limpopo Province, South Africa. PhD Thesis, University of Pretoria, Pretoria, pp.80-112.

International Committee of the Red Cross (ICRC)., 2011. Technical review practical guidelines for test pumping in water wells. Geneva, Switzerland, pp. 31-42.

James, O.B. and Hedenquist, J.W. 1978. Consortium breccia 73255: Petrology of aphanitic lithologies (abs). Lunar Planet. Sci. IX. Lunar Planetary Institute, Houston, pp. 585-587.

Jasmin, I. and Mallikarjuna, P., 2011. Review: Satellite-based remote sensing and geographic information systems and their application in the assessment of groundwater potential, with particular reference to India. *Hydrogeology Journal*, vol. 19(4), pp. 729–740

Javed, A. and Wani, M.H., 2009. Delineation of groundwater potential zones in Kakund watershed, eastern Rajasthan, using remote sensing and GIS techniques. *Journal Geological Society of India*, vol. 73(2), pp. 229-236.

Jensen, M.E. and Haise, H.R., 1963. Estimating evapotranspiration from solar radiation. Proceedings of the American Society of Civil Engineers. *Journal of Irrigation and Drainage*, vol. 89(IR4), pp. 15-41.

Jerez, S., Pedro Montavez, J., Jimenez-Guerrero, P., Jose GomezNavarro, J., Lorente-Plazas, R. and Zorita, E., 2013. A multi-physics ensemble of present-day climate regional simulations over the Iberian Peninsula. *Climate Dynamics*, vol. 40(11-12), pp. 3023–3046.

Jha, M. K. and Chowdary, V. M., 2007. Challenges of using remote sensing and GIS in developing nations. *Hydrogeology Journal*, vol. 15(1), pp. 197-200.

Jha, M.K., Chowdhury, A., Chowdary, V.M. and Peiffer, S., (2007) Groundwater management and development by integrated remote sensing and geographic information systems: prospects and constraints. *Water Resource Management*, vol. 21(2), pp. 427–467.

Jha, M.K., Chowdary, V.M. and Chowdhury, A., 2010. Groundwater assessment in Salboni Block, West Bengal, India using remote sensing, geographical information system and multi-criteria decision analysis techniques. *Hydrogeology Journal*, vol. 18(6), pp. 1713–1728.

Jones, W.S., Panday, S., Frost, S. and McGurk, B., 2003. Surface/subsurface modelling of Western Orange and Seminole Counties of Florida. Proceedings of MODFLOW 2003 and Other Modelling Odysseys, Poeter, Zheng, Hill & Doherty (eds.), Golden, CO, pp. 129-133.

Kollet, S.J. and Maxwell, R.M., 2006. Integrated surface–groundwater flow modeling: A free-surface overland flow boundary condition in a parallel groundwater flow model. *Advances in Water Resources*, vol. 29(7), pp. 945–958.

Krishnamurthy, J. and Srinivas, G., 1995. Role of geological and geomorphological factors in ground water exploration: a study using IRS LISS data. *International Journal of Remote Sensing*, vol. 16(14), pp. 2595-2618.

Krishnamurthy, J.N., Venkatesa, K., Jayaraman, V. and Manivel, M., 1996. An approach to demarcate ground water potential zones through remote sensing and geographical information system. International. *Journal of Remote Sensing*, vol. 17(10), pp. 1867–1884.

Kristensen, K.J. and Jensen, S.E. 1975. A model for estimating actual evapotranspiration from potential evapotranspiration. *Nordic Hydrology*, vol. 6, pp. 170-88.

Kruseman, G.P. and Ridder, N.A., 2000. Analysis and evaluation of pumping test data. ILRI, Wageningen.

Kunstmann, H., Krause, J. and Mayr, S., 2006. Inverse distributed hydrological modelling of Alpine catchments. *Hydrology and Earth System Sciences Discussions*, vol. 10(3), pp. 395-412.

Le Roux, P.A., van Tol, J.J., Kuenene, B.T., Hensley, M., Lorentz, S.A. and Everson, C.S., 2011. Hydropedological interpretations of the soils of selected catchments with the aim of improving the efficiency of hydrological models. *Water Research Commision. Gezina*.

Leavesley, G.H., Lichty, R.W., Troutman, B.M. and Saindon, L.G., 1983. Precipitation-runoff modelling system—User’s Manual: *U.S Geological Survey Water resources Investigations Report* 83-4238, pp. 207.

Leduc, C., Favreau, G. and Schroeter, P., 2001. Long-term rise in a Sahelian water table: the Continental Terminal in southwest Niger. *Journal of Hydrology*, vol. 243, pp. 43–54.

Leek, F., 2006. Hydrogeological characterization of the Palouse basin basalt aquifer system, Washington and Idaho. M.Sc. Thesis (unpublished), Washington State University, Washington, pp. 33.

Lerner, D.N., Issar, A.S. and Simmers, I., 1990. Groundwater recharge, A guide to understanding and estimating natural recharge. Int. *Contributions to Hydrogeology* (IAH), Vol. 8, 1990, Verlag Heinz Heise, Germany, pp. 345.

Lillesand, T., 1990. Special Issue Symposum on Geographic Information Systems. Satellite remote sensing: Its evolution and synergism with GIS technology. *Government Information Quarterly*, vol. 7(3), pp. 307–327.

Litaor, M., Eshel, G., Sade, R., Rimmer, A. and Shenker, M., 2008. Hydrogeological characterization of an altered wetland. *Journal of Hydrology*, vol. 349(3), pp. 333-349.

Liu, H., Chen, X., Bao, A. and Wang, L., 2007. Investigation of groundwater response to overland flow and topography using a coupled MIKE SHE/MIKE 11 modeling system for an arid watershed. *Journal of Hydrology*, vol. 347, pp. 448-459.

Lourens, P.J.H., 2013. The relation between South African geology and geohydrology. M.Sc. Thesis (unpublished), University of the Free State, Bloemfontein, pp. 206 – 212.

Lyle, J. and Stutz, F.P., 1983. Computerised land use suitability mapping. *The Cartographic Journal*, vol. 20(1), pp.39-49.

Machiwal, D., Jha, M.K. and Mal, B.C., 2011. Assessment of groundwater potential in a semi-arid region of India using remote sensing GIS and MCDM techniques. *Water Resources Management*, vol. 25(5), pp. 1359–1386.

Madsen, H., Wilson, G. and Ammentorp H.C., 2002. Comparison of different automated strategies for calibration of rainfall runoff models. *Journal of Hydrology*, vol. 261, pp. 48-59.

Madsen, H., 2003. Parameter estimation in distributed hydrological catchment modelling using automatic calibration with multiple objectives. *Advances in Water Resources*, vol. 26, pp. 205-216.

Magesh, N.S., Chandrasekar, N. and Soundranayagam, J.P., 2012. Delineation of groundwater potential zones in Theni district, Tamil Nadu, using remote sensing, GIS and MIF techniques. *Geoscience Frontiers*, vol. 3(2), pp. 189-196.

Makungo, R., Odiyo, J.O., Ndiritu, J.G. and Mwaka, B., 2010. Rainfall–runoff modelling approach for ungauged catchments: a case study of Nzhelele River subquaternary catchment. *Physics and Chemistry of the Earth*, vol. 35, pp. 596–607.

Marghany, M., Hashim, M. and Mansor S., 2009. Geologic mapping of United Arab Emirates using multispectral remotely sensed data. *American Journal of Engineering and Applied Sciences*, vol. 2(2), pp. 476-480.

Markstrom, S.L., Niswonger, R.G., Regan, R.S., Prudic, D.E. and Barlow, P.M., 2008, GSFLOW coupled groundwater and surface-water flow model based on the integration of the Precipitation-Runoff Modeling System (PRMS) and the Modular Ground-Water Flow Model (MODFLOW-2005): *U.S. Geological Survey Techniques and Methods* 6-D1, pp. 240.

McKeen, S.A., Wilczak, J., Grell, G., Djalalova, I., Peckham, S., Hsie, E., Gong, W., Bouchet, V., Menard, S., Moffet, R., McHenry, J., McQueen, J., Tang, Y., Carmichael, G. R., Pagowski, M., Chan, A., Dye, T., Frost, G., Lee, P. and Mathur, R., 2005. Assessment of an ensemble of seven realtime ozone forecasts over eastern North America during the summer of 2004, *Journal of Geophysical Research*, vol. 110(21), pp. 1984-2012.

Mclin, S.G., 2007. Hydrogeologic characterization of a groundwater system using sequential aquifer tests and flowmeter logs. *New Mexico Geological Society Guidebook*. 58th Field Conference, Jemez Mountains II. pp. 485-491.

Meyer, R., 2002. Guidelines for the monitoring and management of groundwater resources in rural water supply schemes, *Water Research Commission Report* no. 861/1/02a, pp. 55.

Mogaji K. A., Aboyeji, O. S. and Omosuyi, G.O., 2012. Mapping of lineaments for groundwater targeting in basement complex area of Ondo state using remotely sensed data. Department of Applied Geophysics, Federal University of Technology, Akure, Nigeria Regional Centre for Training in Aerospace Surveys (RECTAS).

Mondal S.M., Pandey, A.C. and Garg, R.D., 2008. Groundwater prospects evaluation based on hydrogeomorphological mapping using high resolution satellite images: A case study in Uttarakhand. *Journal of Indian Society of Remote Sensing*, vol. 36 (1), pp. 69-76.

Mook, W.G. (ed.), 2001. UNESCO/IAEA series on environmental isotopes in the hydrological cycle, vol. 6: Available at http://www.nawebh.iaea.org [Accessed 17 November 2014]

Morelli, M. and Piana, F., 2006. Comparison between remote sensed lineaments and geological structures in intensively cultivated hills (Monferrato and Langhe domains, NW Italy). *International Journal of Remote Sensing*, vol. 27(20), pp. 4471−4493.

Moriasi, D.N., Arnold, J.G., Van Liew, M.W., Bingner, R.L., Harmel, R.D. and Veith, T.L., 2007. Model evaluation guidelines for systematic quantification of accuracy in watershed simulations. *Transactions of the ASABE (Soil and Water Division),* vol. 50(3), pp. 885-900.

Morris, B.L., Lawrence, A.R.L., Chilton, P.J.C., Adams, B., Calow, R.C. and Klinck, B.A., 2003. Groundwater and its susceptibility to degradation: A global assessment of the problem and options for management. Early warning and assessment report series, RS. 03-3. *United Nations Environment Programme*, Nairobi, Kenya.

Mukherjee, P., Singh, C.K. and Mukherjee S., 2012. Delineation of groundwater potential zones in arid region of India - A remote sensing and GIS approach. *Water Resources Management*, vol. 26(9), pp. 2643–2672.

Nagarajan, M. and Singh. S., 2009. Assessment of groundwater potential zones using GIS technique. *Journal of the Indian Society of Remote Sensing*, vol. 37(1), pp. 69-77.

Nash, J.E. and Sutcliffe, J.V., 1970. River flow forecasting through conceptual models part I - A discussion of principles. *Journal of hydrology*, vol. 10(3), pp. 282-290.

National Remote Sensing Agency (NRSA), 2008. Groundwater prospects mapping using remote sensing and geographic information systems, Rajiv Gandhi national drinking water mission project manual, pp. 256.

Nealer, E.J., Betram, E., van Eaden, E., van Niekerk, D., Tempelhoff, J. and Coetzee, C., 2009. Addressing issues of epidemiological disaster: observations on the Delmas water-based crises: 1993-2007. Version 1. Research Report. South African National Disaster Management Centre (SANDMC).

Nemaxwi, P., 2016. Estimation of groundwater recharge response from rainfall events in a semi-arid fractured aquifer: Case study of quaternary catchment A91H, Limpopo Province, South Africa. M.Sc. Thesis (unpublished), University of Venda, Thohoyandou, pp. 61.

Nguyet, V.T.M., 2006. Hydrogeological characterisation and groundwater protection of tropical mountainous karst areas in NW Vietnam: V U B – Hydrologie. Brussel. Department of Hydrology and Hydraulic Engineering.

Nkondo, M.N., van Zyl, F.C., Keuris, H. and Schreiner, B., 2012. Draft national water resource strategy 2 (NWRS-2). *Department of Water Affairs and Forestry. Pretoria*, pp. 150.

Odiyo, J.O., Phangisa, J.I. and Makungo, R., 2012. Rainfall–runoff modelling for estimating Latonyanda River flow contributions to Luvuvhu River downstream of Albasini Dam. *Physics and Chemistry of the Earth, Parts A/B/C*, vol. 50, pp.5-13.

O'Leary, D.W., Friedman, J.D. and Pohn, H.A., 1976. Lineament, linear, lineation: Some proposed new standards for old terms. *Geological Society America Bulletin*, vol. 87, pp. 1463-1469.

Panday, S. and Huyakorn, P.S., 2004. A fully coupled physically-based spatially-distributed model for evaluating surface/subsurface flow. *Advances in Water Resources*, vol. 27(4), pp. 361-382.

Park, H.Y., Jang, K., Ju, J.W. and Yeo, I.W., 2012. Hydrogeological characterization of seawater intrusion in tidally-forced coastal fractured bedrock aquifer. *Journal of Hydrology* vol. 446(7), pp. 77–89.

Pietersen, K., Beekman, H.E. and Holland, M., 2011. South African groundwater governance case study. World Bank, *South African Department of Water Affairs and Water Research Commission.* WRC Report No. KV 273/11, pp. 19.

Pinto, D., Shrestha, S., Babel, M.S. and Ninsawat, S., 2015. Delineation of groundwater potential zones in the Comoro watershed, Timor Leste using GIS, remote sensing and analytic hierarchy process (AHP) technique. *Applied Water Science*, pp.1-17.

Pradeep, R., 1998. Remote sensing techniques to locate groundwater potential zones in upper Urmil River Basin, District Chhatarpur—Central India. *Journal of the Indian Society of Remote Sensing*, vol. 26(3), pp. 135–147.

Pradhan, B., 2009. Groundwater potential zonation for basaltic watersheds using satellite remote sensing data and GIS techniques. *Central European Journal of Geosciences*, 1(1), pp. 120-129.

Prasad, R.K., Mondal, N.C., Banerjee, P., Nandakumar, M.V. and Singh, V.S., 2008. Deciphering potential groundwater zone in hard rock through the application GIS. *Environmental Geology*, vol. 55, pp. 467–475.

Rao, Y.S. and Jugran, D.K., 2003. Delineation of groundwater potential zones and zones of groundwater quality suitable for domestic purposes using remote sensing and GIS. *Hydrological Sciences Journal*, vol. 48(5), pp. 821–833.

Refsgaard, J.C. and Storm, B., 1995. MIKE SHE. *Computer models of watershed hydrology*, vol. 1, pp. 809-846.

Robinson, G.M., Gray, D.A., Healey, R.G. and Furley, P.A., 1989. Developing a geographical information system (GIS) for agricultural development in Belize, Central America. *Applied Geography*, vol. 9(2), pp. 81–94.

Saaty, T.L., 1980. The analytic hierarchy process: planning, priority setting, resource allocation. New York: McGraw-Hill.

Sander, P., 2007. Lineaments in groundwater exploration: a review of applications and limitations. *Hydrogeology Journal*, vol. 15(1), pp. 71–74.

Sandu, M.A. and Virsta, A., 2015. Applicability of MIKE SHE to simulate hydrology in Argesel River Catchment. *Agriculture and Agricultural Science Procedia*, vol. 6, pp. 517-524.

Santhi, C., Arnold, J. G., Williams, J. R., Dugas, W. A., Srinivasan, R. and Hauck, L. M., 2001. Validation of the SWAT model on a large river basin with point and nonpoint sources. *Journal of American Water Resources Association*, vol. 37(5), pp. 1169-1188.

Sami, K. and Hughes, D.A., 1996. A comparison of recharge estimates to a fractured sedimentary aquifer in South Africa from a chloride mass balance and an integrated surface-sub-surface model. *Journal of Hydrology*, vol. 179, pp. 111-136.

Selaolo, E.T., 1998. Tracer studies and groundwater recharge assessment in the eastern fringe of the Botswana Kalahari - The Letlhakeng-Botlhapatlou area. PhD Thesis, Free University (Amsterdam), pp. 229.

Senanayake, I.P., Dissanayake, D.M.D., Mayadunna, B.B. and Weerasekera, W.L., 2016. An approach to delineate groundwater recharge potential sites in Ambalantota, Sri Lanka using GIS techniques. *Geoscience Frontiers*, vol. 7(1), pp. 115-124.

Shalini, O., 2006. Runoff simulation in the Canagagigue creek watershed using the MIKE SHE model. M.A.Sc Thesis (unpublished), McGill University, Montreal, Canada, pp. 65.

Shamsudin, S. and Hashim, N., 2002. Rainfall runoff simulation using MIKE 11 NAM. Journal of civil engineering, vol. 15(2), pp. 1-13.

Singh, J., H. V. Knapp, and M. Demissie. 2004. Hydrologic modeling of the Iroquois River watershed using HSPF and SWAT. ISWS CR 2004-08. Champaign, Ill.: Illinois State Water Survey, pp. 343-360.

South African Committee for Stratigraphy (SACS), 1980. Stratigraphy of South Africa. Part 1 (Compiled by L.E. Kent). Lithostratigraphy of the Republic of South Africa, Namibia, and Republics of Bophuthatswana, Transkei and Venda. Handbook of geological surveys in South Africa, pp. 690.

Sreedhar, G., Vijaya Kumar, G.T., Murali Krishna, I.V., Ercan, K. and Cüneyd, D.M., 2009. Mapping of groundwater potential zones in the Musi basin using remote sensing data and GIS. *Advances in Engineering Software*, vol. 40(7), pp. 506–518.

Sreela, R., Girish, G., Reji, S., Rajesh, R. and Kurian, S., 2013. Demarcation of groundwater prospective zones in humid tropical river basin: A geospatial approach. *Iranian Journal of Earth Sciences*, vol. 5(1), pp. 1-12.

Taylor, C.J. and Greene, E.A., 2006. Hydrogeologic characterization and methods used in the investigation of karst hydrology. Chapter 3. In: Rosenberry, D.O. and LaBaugh, J.W. Eds. Field techniques for estimating water fluxes between surface water and ground water Techniques and Methods 4–D2. U.S. *Geological Survey*, pp. 75-107.

Thakur, R. and Sharma, M., 2009. GIS and challenges to planning and development applications in peripheral regions. In: Gatrell, J. and Jensen, R. Eds. Geotechnologies and the Environment: Planning and socioeconomic applications. Heidelberg: Springer. pp. 125-137.

Theis, C.V., 1935. The relation between the lowering of the piezometric surface and the rate and duration of discharge of a well using groundwater storage: *Transactions of the American Geophysical Union*, vol. 16(2), pp. 519–524.

Therrien, R., Sudicky, E.A. and McLaren, R.G., 2004. An efficient simulator for three-dimensional, saturated- unsaturated groundwater flow and density dependent, chain decay solute transport in porous, discretely fractured porous or dual porosity formations. *Groundwater Simulations Group*, Waterloo, Ontario, pp. 138.

Thompson, J.R., Sorenson, H.R., Gavin, H. and Refsgaard, A., 2004. Application of the MIKE SHE/MIKE 11 modelling system to a lowland wet grassland in southeast England. *Journal of Hydrology*, vol. 293(1-4): 151-179.

Thornthwaite, C.W., 1948. An approach toward a rational classification of climate. *Geographical review*, vol. 38(1), pp. 55-94.

UNEP/DEWA (United Nations Environment Programme Division of Early Warning and Assessment), 2002. A survey of methods for groundwater recharge in arid and semi-arid regions. ISBN 92-80702131-3, Nairobi, Kenya: UNEP/DEWA.

Van Camp, M., Mjemah, I. C., Al Farrah, N. and Walraevens, K., 2013. Modeling approaches and strategies for data-scarce aquifers: example of the Dar es Salaam aquifer in Tanzania. *Hydrogeology Journal*, vol. 21(2), pp. 341-356.

Van der Lee, J. and Gehrels, J.C., 1997. Modelling of groundwater recharge for a fractured dolomite aquifer under semi-arid conditions. In IAH-Recharge of Phreatic Aquifers in Semi-Arid Areas (ed. I. Simmers), A.A. Balkema/Rotterdam: pp. 129-144.

Van Liew, M. W., Arnold, J. G. and Garbrecht, J. D., 2003. Hydrologic simulation on agricultural watersheds: Choosing between two models. *Transactions of the ASAE*, vol. 46(6), pp. 1539-1551.

Van Tonder, G.J., Botha, J.F., Chiang, W.H., Kunstmann, H. and Xu, Y., 2001. Estimation of the sustainable yields of boreholes in fractured rock formations. *Journal of Hydrology*, vol. 241, pp. 70-90.

Van Tonder, G., Bardenhagen, I., Riemann, K., Bosch, K.R.J., Dznanga, P. and Xu, Y., 2002. Manual on pumping test analysis in fractured-rock aquifers: *WRC Report* No. 1116/1/02, pp. 16.

Van Wyk, E., van Tonder, G.J. and Vermeulen, D., 2012. Characteristics of local groundwater recharge cycles in South African semi-arid hard rock terrains: Rainfall–groundwater interaction. *Water SA*, vol. 38(5), pp. 747-754.

Vasanthavigar, M., Srinivasamoorthy, K., Vijayaragavan, K., Gopinath, S. and Sarma, S., 2011. Groundwater Potential Zoning in Thirumanimuttar Sub-Basin Tamilnadu, India—A GIS and Remote Sensing Approach. *Geo-spatial Information Science*, vol. 14(1), pp. 17-26.

Vazquez, R.F., Willems, P. and Feyen, J., 2008. Improving the predictions of MIKE SHE catchment-scale application by using a multi-criteria approach. *Hydrological Processes*, vol. 22, pp. 2159-2179.

Weaver, J.M.C. and Talma, A.S., 1999. Field studies of chlorofluorocarbons (CFC's) as a groundwater dating tool in fractured rock aquifers, Pretoria, *WRC* Report 731/1/99.

Weber, M., Gordon, S., Judd-Henrey, I. and Beckers, J., 2004. Management strategies to reduce vulnerability to climate change in the South Saskatchewan River Basin. Alberta Research Council.

White, W.B., 1999, Conceptual models for karstic aquifers. In: Palmer, A.N. Palmer, M.V. and Sasowsky, I.D., 1999. Eds., Karst modeling: Karst Waters Institute Special Publication. Leesburg, Virginia, vol. 5, pp. 11–16.

Worldwide Hydrogeological Mapping and Assessment Programme (WHYMAP), 2008. Groundwater resources map of Africa, BGR, Hannover, Germany and UNESCO, Paris. Available at http://www.whymap.org/. [Accessed 15 Dec 2008]

World Weather Online (WWO), 2014. Giyani weather South Africa. [online] Available at: http://www.worldweatheronline.com/Giyani-weather/Limpopo/ZA.aspx[Accessed 04 May 2014]

Xevi, E., Christiaens, K., Espino, A., Sewnandan, W., Mallants, D., Sørensen, H. and Feyen. J., 1997. Calibration, validation and sensitivity analysis of the MIKE-SHE Model using the

Neuenkirchen Catchment as case study. *Water Resources Management*, vol. 11(3), pp. 219–242.

Xu, Y. and van Tonder, G.J., 2001. Estimation of recharge using a revised CRD method. *Water SA*, vol. 27(3), pp. 341-343.

Xu, Y., Titus, R., Holness, S.D., Zhang, J. and van Tonder, G.J., 2002. A hydrogeomorphological approach to quantification of groundwater discharge to streams in South Africa. *Water SA*, vol. 28(4), pp. 375-380.

Xu, Y. and Beekman, H.E. (Eds)., 2003. Groundwater recharge estimation in Southern Africa. UNESCO IHP Series No. 64, UNESCO Paris. ISBN 92-9220-000-3.

Xu, Y., Lin, L. and Jia, H., 2009. Groundwater flow conceptualization and storage determination of the Table Mountain Group (TMG) Aquifers. Water Research Commission. *WRC Report* No. 1419/1/09, pp. 261.

Yan, J.S. and Smith, K.R., 1994. Simulation of integrated surface-water and ground-water systems: Model formulation. *Water Resources Bulletin*, vol. 30, pp. 879–890.

# APPENDICES

## Appendix A

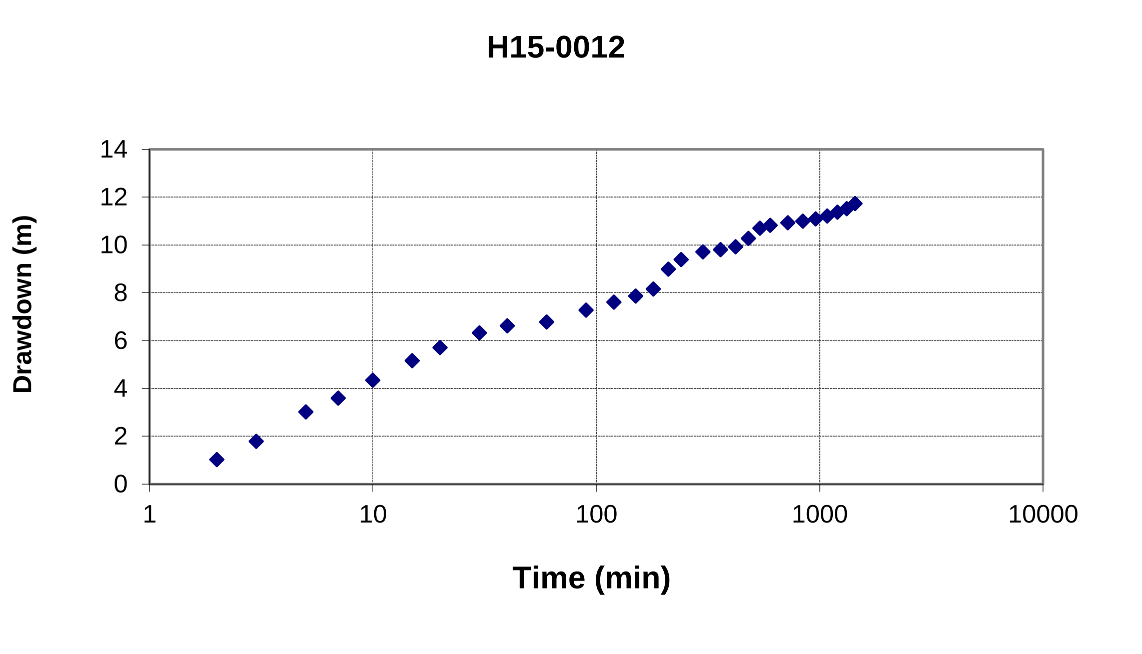


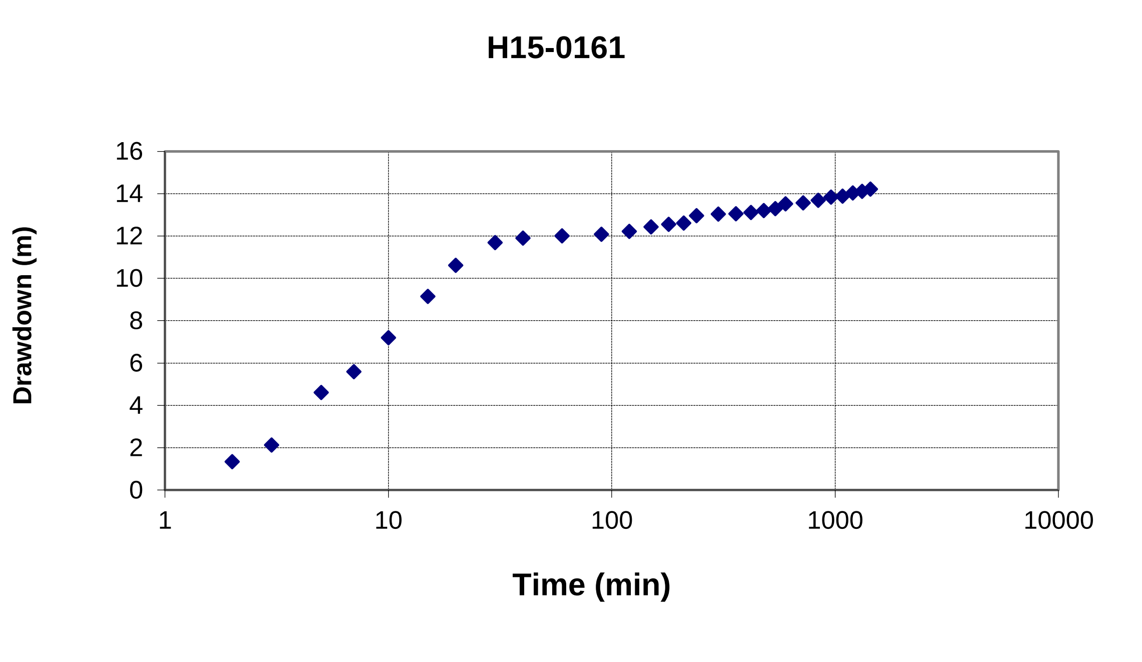

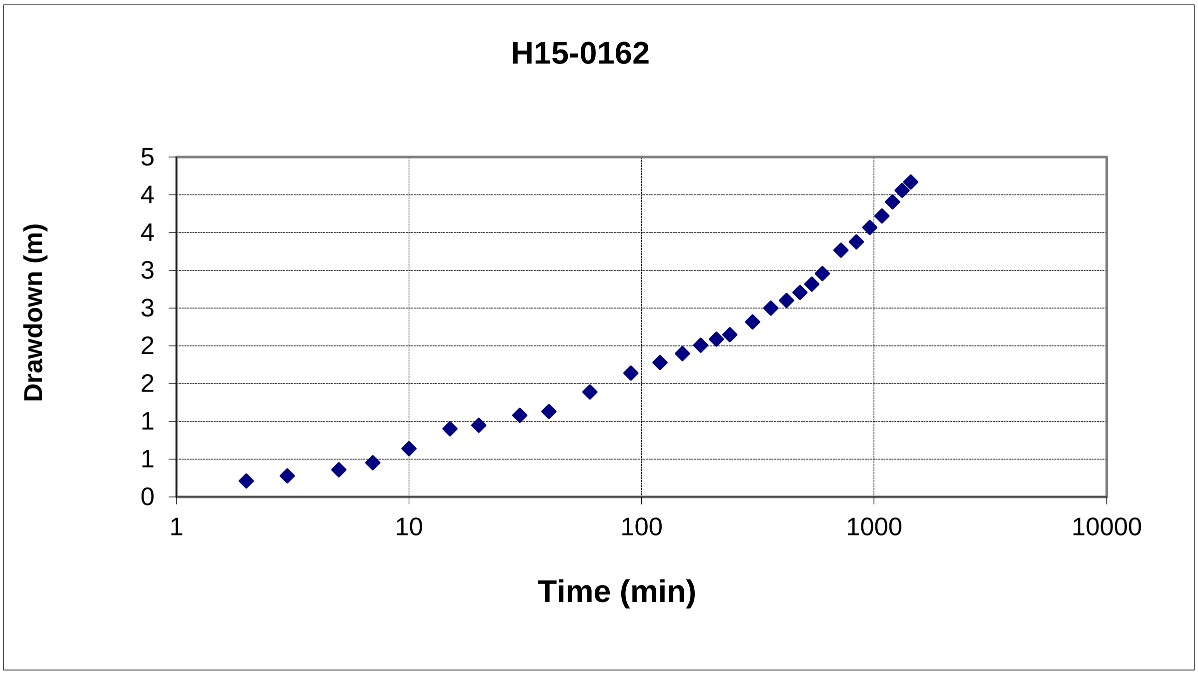

H15-0162
Drawdown (m)
5
4
4
3
3
2
2
1
1
0
1
10
100
1000
10000
Time (min)


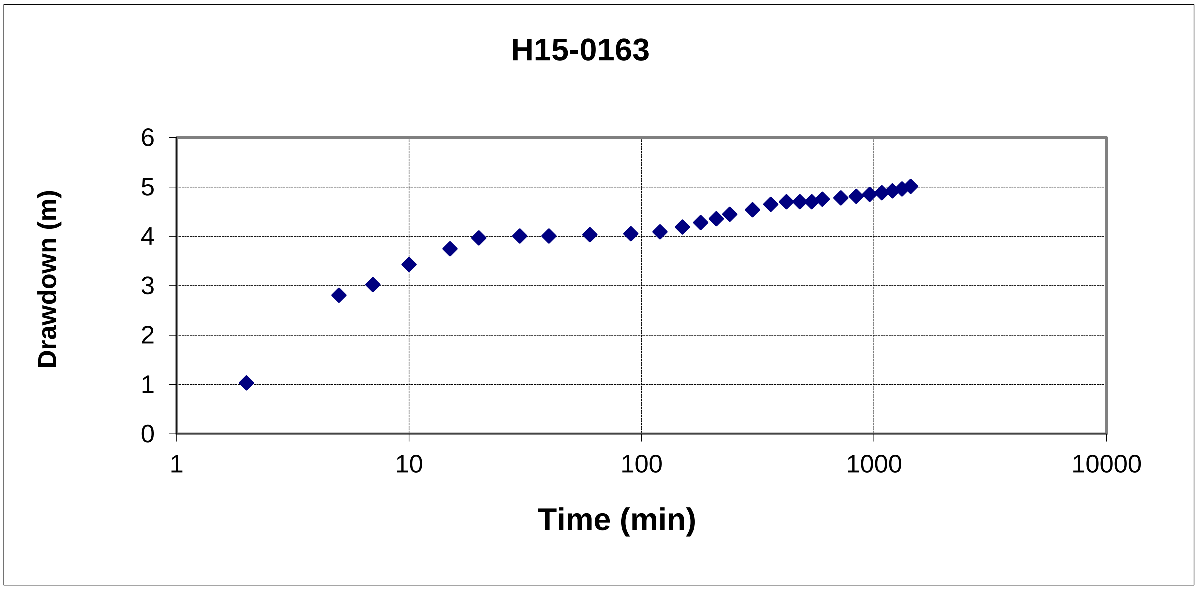

H15-0163
Drawdown (m)
6
5
4
3
2
1
0
1
10
100
1000
10000
Time (min)

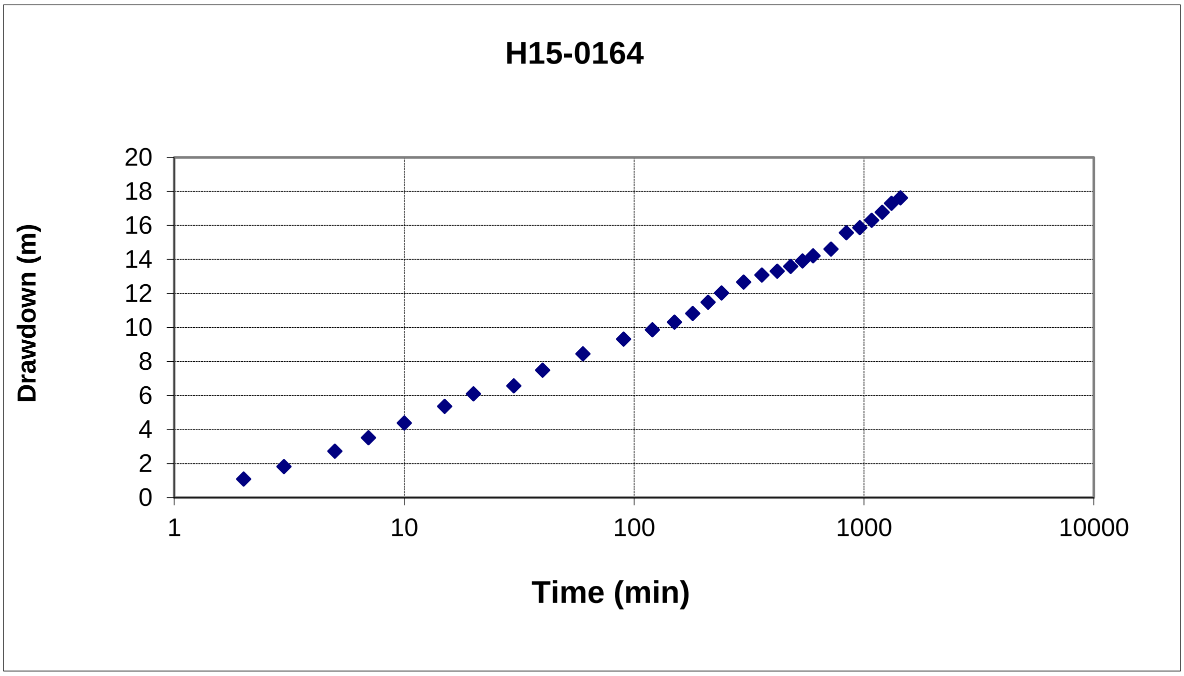
H15-0164
Drawdown (m)
20
18
16
14
12
10
8
6
4
2
0
1
10
100
1000
10000
Time (min)

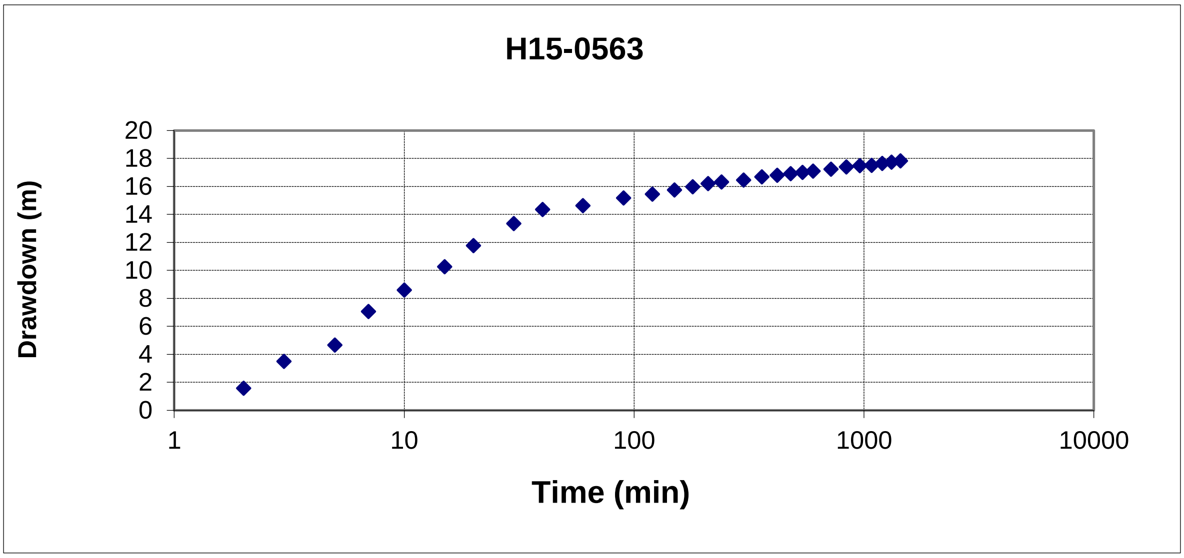
H15-0563
Drawdown (m)
20
18
16
14
12
10
8
6
4
2
0
1
10
100
1000
10000
Time (min)

# Appendix B

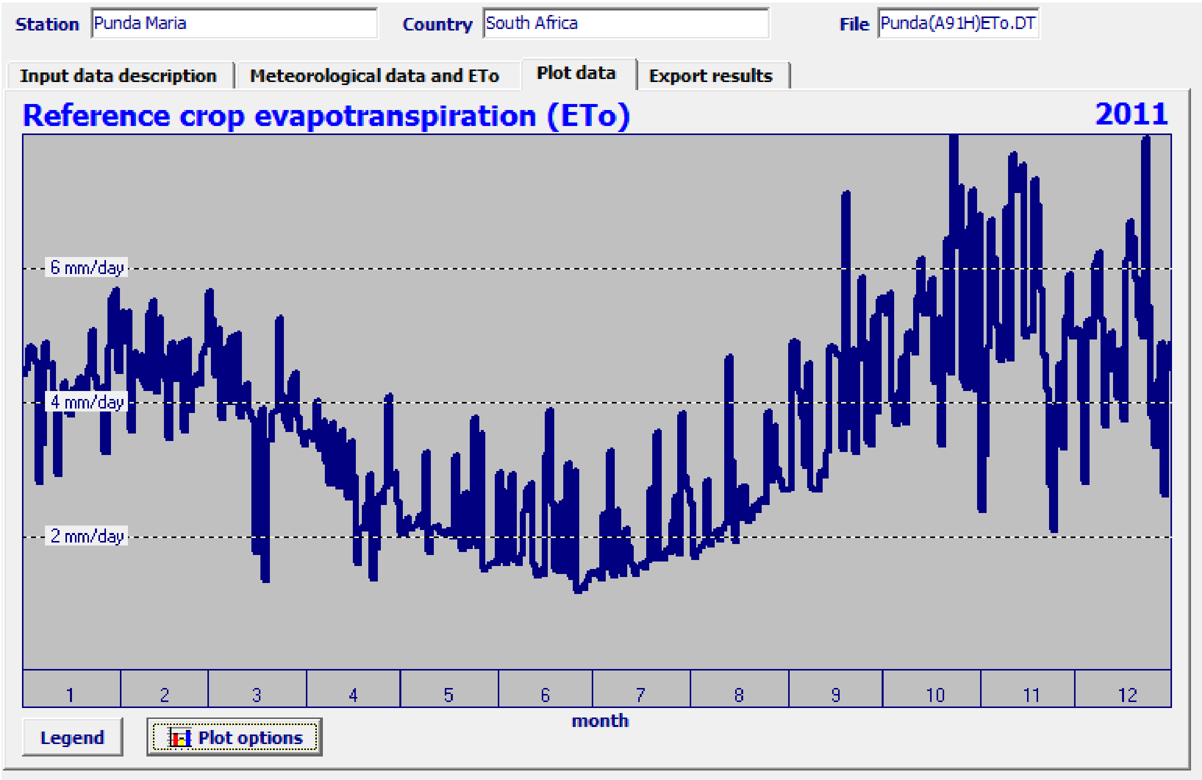
Station Punda Maria
Country South Africa
File Punda(A91H)ETo.DT
Input data description
Meteorological data and ETo
Plot data
Export results
Reference crop evapotranspiration (ETo)
2011
6 mm/day
4 mm/day
2 mm/day
1
2
3
4
5
6
7
8
9
10
11
12
month
Legend
Plot options

# Appendix C

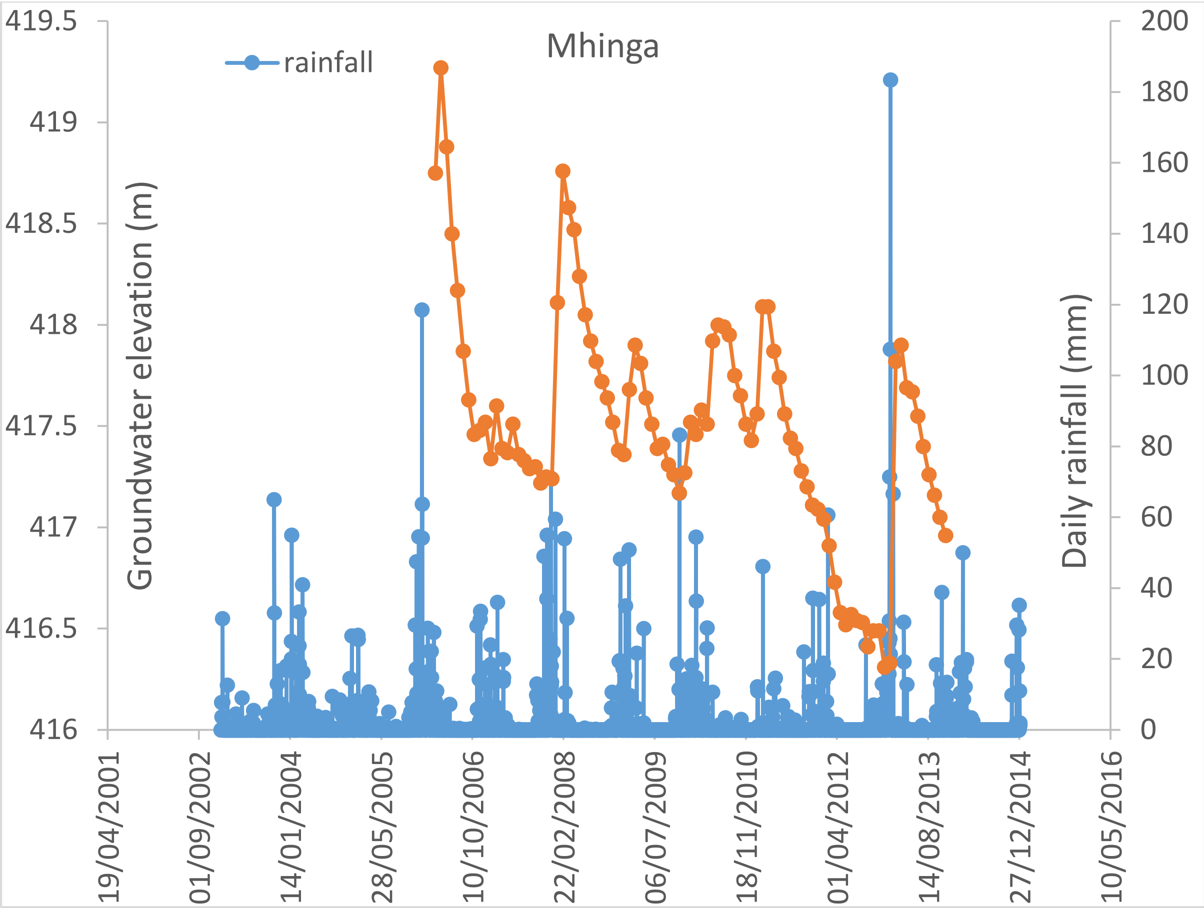
Mhinga
rainfall
Groundwater elevation (m)
Daily rainfall (mm)
419.5
419
418.5
418
417.5
417
416.5
416
200
180
160
140
120
100
80
60
40
20
0
19/04/2001
01/09/2002
14/01/2004
28/05/2005
10/10/2006
22/02/2008
06/07/2009
18/11/2010
01/04/2012
14/08/2013
27/12/2014
10/05/2016